

# Functional sets with typed symbols: Framework and mixed Polynotopes for hybrid nonlinear reachability and filtering. \*

C. Combastel <sup>a</sup>

<sup>a</sup> Univ. Bordeaux, CNRS, IMS, UMR 5218, 33405 Talence, France

---

## Abstract

Verification and synthesis of Cyber-Physical Systems (CPS) are challenging and still raise numerous issues so far. In this paper, an original framework with mixed sets defined as function images of symbol type domains is first proposed. Syntax and semantics are explicitly distinguished. Then, both continuous (interval) and discrete (signed, boolean) symbol types are used to model dependencies through linear and polynomial functions, so leading to mixed zonotopic and polynotopic sets. Polynotopes extend sparse polynomial zonotopes with typed symbols. Polynotopes can both propagate a mixed encoding of intervals and describe the behavior of logic gates. A functional completeness result is given, as well as an inclusion method for elementary nonlinear and switching functions. A Polynotopic Kalman Filter (PKF) is then proposed as a hybrid nonlinear extension of Zonotopic Kalman Filters (ZKF). Bridges with a stochastic uncertainty paradigm are outlined. Finally, several discrete, continuous and hybrid numerical examples including comparisons illustrate the effectiveness of the theoretical results.

**Key words:** Functional sets; Polynomial dependencies; Mixed encoding; Logic; Hybrid dynamic systems; Reachability; Robust state estimation; Kalman filters; Zonotopes; Polynotopes;

---

## 1 Introduction

Uncertainty management undoubtedly remains a great challenge when designing, observing, controlling and verifying systems with stringent safety, reliability and accuracy requirements. Trials and errors are inherent to any innovation process, even if correct-by-design methodologies tend to reduce the number of iterations. Common industrial practice still makes intensive use of Monte-Carlo simulations [34] and design of experiments [56] to check for robustness, perform sensitivity analysis and optimize tuning. Meanwhile, given some model of the available knowledge, which is by essence subject to uncertainties, formal methods [7] provide verification and synthesis tools likely to ensure a full coverage wrt to the range of specified behaviors, including off-nominal and worst cases. Dealing with complex dynamics such as

nonlinear and hybrid ones remains challenging and the achieved trade-off between computation time and accuracy heavily depends on underlying set representations.

### 1.1 Problem setting and antecedents

Within the set-membership literature, intervals [51,29], ellipsoids [66,43,36] and polytopes [74,26] have initiated a growing body of research works addressing the core problem of reachability [52,23,39,42,61,15,68,3,5,41,6,25], but also possibly distributed [54,53,17] state estimation [57,1,9,10,11,37,71,13,14,44,59,64,2,60,19,18], identification [47,8], computation of invariant sets [20,46,72], fault diagnosis [16,73,12,69,58,55], among others. Intervals (resp. ellipsoids) are not closed under linear maps (resp. Minkowski sum) and basic polytope computations do not scale very well. Those sets, and convex sets in general, can be represented by support functions [38]. Dealing with non convex and/or non-connected sets is still possible through pavings [29] and/or bundles [50,4] but costly since related algorithms often rely on bisections yielding an exponential complexity. Level sets [49] also constitute an alternative which suffers from the curse of dimensionality. Moreover, a direct use of set-membership techniques is often subject to the so-called dependency problem due to the loss of variable multi-occurrences when overloading basic operators like sum,

\* This paper was not presented at any IFAC meeting. Corresponding author: C. Combastel. Tel: +33 5 40 00 25 25.

Email address: christophe.combastel@u-bordeaux.fr (C. Combastel).

<sup>1</sup> This study has been carried out with financial support from the French State, managed by the French National Research Agency (ANR) in the frame of the “Investments for the future” Programme IdEx Bordeaux - SysNum (ANR-10-IDEX-03-02).

difference, product, etc. This may yield pessimistic evaluations leading to the so-called wrapping effect [35,40] when uncertainty propagation through dynamic systems is considered. This has motivated the use of affine arithmetic [21,65] and other set representations of intermediate complexity between interval/ellipsoids and polytopes/level sets, like zonotopes. Zonotopes form a class of convex and centrally symmetric polytopic sets defined as the affine image of a unit hypercube [35,9,24]. Then, affine function transforms correspond to implicit set operations and the evaluation of bounds can be delayed (lazy evaluation [70]), to the benefit of a better management of (linear) dependencies.

At this step, an analogy can be noticed between such affine function transforms and the manipulation of symbolic expressions at a syntactic level (e.g.  $x - x$  simplified as 0 before substituting the unit interval  $[-1, +1]$  for  $x$  in  $x - x$ ). In addition, a distinction can be made between syntax (e.g. formal transformation rules) and semantics (e.g. the set-valued interpretation of some expression). This important distinction is not always visible with sets, notably if, e.g., the zonotope  $\langle c, R \rangle = \{x = c + Rs, s \in [-1, +1]^p\} \subset \mathbb{R}^n$  is identified with the pair  $(c, R)$  and/or the formal expression  $c + Rs$  defining an affine function of symbolic variables in  $s$ . This motivated the recent introduction of symbolic zonotopes and USP (Unique Symbol Provider) in [17]. To summarize, a clear distinction between syntax and semantics appears as a key point to struggle against the dependency problem in set-membership computations. This distinction, usual in other fields like mathematical logic [62], will serve as a guideline to set-up the generic framework of image-sets introduced in this paper.

Though zonotopic sets catch some linear dependencies with their generators (i.e. columns of  $R$ ), their convex, connected, and centrally symmetric nature still impose restrictions to address the reachability of nonlinear and hybrid (i.e. mixed continuous/discrete) dynamic systems. To overcome these restrictions, Taylor models [42], polynomial zonotopes [3] and sparse polynomial zonotopes (spz) [32] rely on sets defined as polynomial images rather than affine/linear ones. Constraints can be also introduced in the set representation as with constrained zonotopes [69] and, very recently, constrained polynomial zonotopes [33]. Note that the evaluation of bounds under constraints, even if delayed, may be costly and involve iterative algorithms (e.g. linear programming with constrained zonotopes).

## 1.2 Contributions and related organization

In this paper, after preliminaries (section 2), a different approach is explored to gather in a single data structure the representation of possibly non-convex and non-connected sets: Symbol typing, while keeping the general idea of defining sets as the image of a domain

by a function.

Indeed, the proposed framework of functional sets with typed symbols (section 3) does not impose a priori restrictions on the class of functions which may be linear (zonotopes), polynomial (polynotopes) or any others. As already mentioned, the distinction between syntax and semantics will be explicitly formalized (notation:  $\iota$  for “interpretation of”). Moreover, the definition domain of the function used to define an image set will depend on the type of the symbolic variables formalizing the function inputs. A compact and dependency preserving representation of mixed sets is so obtained. Symbol types are not imposed in the general framework and may include random variables.

Then, special attention is paid to the types unit interval ( $\in [-1, +1]$ ), signed ( $\in \{-1, +1\}$ ) and boolean ( $\in \{0, 1\}$ ) under linear and polynomial dependencies in section 4. For example,  $\{x = c + Rs, s \in [[-1, +1]^c; \{-1, +1\}^d]\}$  defines a mixed zonotope. Mixed polynotopes and mixed image sets are defined as well. Also, an original mixed encoding of intervals is proposed, making it possible to tune the granularity level of the discrete/symbolic part of a mixed representation while avoiding the need for costly bisections/splitting in reachability computations.

In section 5, modeling tools for nonlinear hybrid systems are given with emphasis placed on a compositional approach relying on basic logic gates and basic nonlinear continuous and switching functions. The polynomial representation of logic functions defined on  $\{-1, +1\}$  (signed logic) or  $\{0, 1\}$  (boolean logic) is analyzed and a functional completeness result is given for polynotopes. Inclusion methods are also given.

Then, a Polynotopic Kalman Filter (PKF) extending Zonotopic Kalman Filters (ZKF) to hybrid nonlinear systems is developed in section 6. Through basic operators/functions overloading, its implementation can benefit from the proposed dependency preserving compositional inclusion methods. Moreover, the links between PKF, ZKF and the basic stochastic Kalman Filter KF [30] are made explicit.

In section 7, several numerical examples including comparisons illustrate the effectiveness of the proposed scheme, and concluding remarks are given in section 8.

## 2 Preliminaries

To begin with, a definition of sets from functions (imset) and a definition of inclusion functions are given and discussed in a classical (non-symbolic) framework.

**Definition 1 (imset)** *Given a function  $f : \mathbb{X} \rightarrow \mathbb{Y}$ ,  $x \mapsto y = f(x)$  and a set  $X \subset \mathbb{X}$ , the imset of  $X$  by  $f$  is:*  

$$f(X) = \{f(x) \mid x \in X\}.$$

**Definition 2 (Inclusion function)** *The function  $g : [\mathbb{X}] \rightarrow [\mathbb{Y}]$ ,  $X \mapsto Y = g(X)$  is an inclusion function for the function  $f : \mathbb{X} \rightarrow \mathbb{Y}$ ,  $x \mapsto y = f(x)$  if  $\mathbb{X} \in [\mathbb{X}]$  and:*

$\forall X \in [\mathbb{X}], f(X) \subset g(X)$ ,  
where  $f(X)$  is the imset of  $X \subset \mathbb{X}$  by  $f$ .

**Corollary 3** Since  $[\mathbb{X}]$  must satisfy  $\forall X \in [\mathbb{X}], X \subset \mathbb{X}$ ,  $g$  is an inclusion function for  $f$  if:

$(\mathbb{X} \in [\mathbb{X}]) \wedge \forall X \in [\mathbb{X}], ((X \subset \mathbb{X}) \wedge (f(X) \subset g(X)))$ .  
Notice that  $x \in \mathbb{X}$  is not necessarily set-valued, whereas  $X \in [\mathbb{X}]$  is. For instance,  $[\mathbb{X}]$  may be the set of intervals included in an interval  $\mathbb{X}$  defined on some continuous and/or discrete domain. In the continuous case, the definition 2 is equivalent to that classically used for interval arithmetic.

**Corollary 4**  $\text{imset}_f : [\mathbb{X}] \rightarrow [\mathbb{Y}], X \mapsto Y = f(X)$  is monotone wrt inclusion:  $X_1 \subset X_2 \Rightarrow \text{imset}_f(X_1) \subset \text{imset}_f(X_2)$ . However, it is not required that  $g$  has to be monotone wrt inclusion to be an inclusion function. Even without this requirement, it can be inferred that:

$$\forall X \in [\mathbb{X}], f(X) \subset g(\mathbb{X}).$$

Indeed, from the definition 2,  $\forall X \in [\mathbb{X}], X \subset \mathbb{X}$ , and the monotony of  $\text{imset}_f$  wrt inclusion gives:  $\forall X \in [\mathbb{X}], f(X) \subset f(\mathbb{X})$ . Also, since  $\mathbb{X} \in [\mathbb{X}]$ ,  $f(\mathbb{X}) \subset g(\mathbb{X})$ . Thus,  $\forall X \in [\mathbb{X}], f(X) \subset g(\mathbb{X})$ , without requiring the additional statement that  $g$  must be monotone wrt inclusion to be an inclusion function.

### 3 Framework: Image-sets with typed symbols

A framework for functional sets, that is, sets defined and operated through functions is introduced in this section. With the ultimate goal of better managing dependencies that constitute a key for an accurate propagation of uncertainties, an explicit distinction between syntax and semantics is considered. Whereas syntax refers to rules defining symbol combinations that are correct in some language, semantics refers to the interpretation or meaning of related sentences. In other words, syntax refers to how writing correct statements, semantics indicates what they mean. The proposed framework introduces the so-called image-sets as set-valued interpretations/evaluations (semantics) of functions defined from symbolic expressions (syntax) on some domains. These domains which may be continuous, discrete or mixed, are built from different types of symbolic variables. Moreover, following [17], each of these symbols are uniquely identified in order to preserve dependencies.

#### 3.1 Uniquely identified typed symbols

Let  $\mathbb{I}$  and  $\mathbb{S}$  be two sets, namely a set of identifiers and a set of distinct symbols (symbolic variables). Let  $s$  be a bijective function such that  $s : \mathbb{I} \rightarrow \mathbb{S}, i \mapsto s_i = s(i)$ . This establishes a family of unique symbols in  $\mathbb{S}$  each indexed by a unique identifier in  $\mathbb{I}$ . Moreover,  $s^{-1}(s_i) = i$ , that is, the inverse function  $s^{-1}$  returns the unique identifier of any symbol in  $\mathbb{S}$ . Let  $I \subset \mathbb{I}$ ,  $s_I$  denotes the column vector  $[s_i]_{i \in I}$  made of the symbolic variables identified by  $I$ .

In terms of syntax, each symbol in  $\mathbb{S}$  has a type in  $\mathbb{T}$ . The type assignment function (taf)  $\tau : \mathbb{S} \rightarrow \mathbb{T}, v \mapsto \tau(v)$  assigns a type, possibly empty if unspecified, to each symbol in  $\mathbb{S}$  i.e. to each symbolic variable  $v \in \mathbb{S}$ .

In terms of semantics, each type in  $\mathbb{T}$  can be interpreted as a domain (of possible values) in  $\mathbb{D}$ . The interpretation of a type  $t \in \mathbb{T}$  as a domain is formalized through a bijective function  $\iota_{\mathbb{T}}$  shortly denoted  $\iota$  and defined as  $\iota : \mathbb{T} \rightarrow \mathbb{D}, t \mapsto \iota(t)$ .

Similarly, an interpretation/evaluation<sup>2</sup> of any symbol in  $\mathbb{S}$  as a (possibly set-)value in  $\mathbb{V}$  is formalized through a function  $\iota_{\mathbb{S}}$  shortly denoted  $\iota$  and defined as  $\iota : \mathbb{S} \rightarrow \mathbb{V}, s_i \mapsto \iota(s_i)$ .

A single-valued (resp. set-valued) interpretation  $\iota_{\mathbb{S}}$  of symbols in  $\mathbb{S}$  remain consistent with the interpretation  $\iota_{\mathbb{T}}$  of their types in  $\mathbb{T}$  if<sup>3</sup>:

$$\begin{aligned} \forall i \in \mathbb{I}, \iota(s_i) &\in \iota(\tau(s_i)) \text{ for single-valued,} \\ \forall i \in \mathbb{I}, \iota(s_i) &\subset \iota(\tau(s_i)) \text{ for set-valued.} \end{aligned}$$

In each case, the left (resp. right) occurrence of  $\iota$  refers to the interpretation of symbols  $\iota_{\mathbb{S}}$  (resp. types  $\iota_{\mathbb{T}}$ ). The single-valued or set-valued nature of a symbol interpretation depends on whether the elements of  $\mathbb{V}$  are elements or subsets of  $\mathbb{T}$ . Shorthand notation:  $\iota s_i = \iota(s_i)$ .

**Example 5** Let  $\mathbb{I} = \mathbb{N}$ , that is, the natural integers are used as unique identifiers for symbols (symbolic variables) in  $\mathbb{S}$ . Let  $\mathbb{T} = \{\emptyset, \mathbf{i}, \mathbf{s}, \mathbf{b}\}$  define a set of types where  $\emptyset, \mathbf{i}, \mathbf{s}, \mathbf{b}$  respectively refer to unspecified, interval, signed, boolean. Let shorthand notations for basic domains be defined as  $\square = [-1, +1], |\pm| = \{-1, +1\}, |\mathbf{0}| = \{0, 1\}$ . Let  $\mathbb{D} = \{\emptyset, \square, |\pm|, |\mathbf{0}|^1\}$  denote a set of domains used to interpret the symbol types in  $\mathbb{T}$  through the bijective interpretation function  $\iota$  defined as:

$$\iota(\emptyset) = \emptyset, \iota(\mathbf{i}) = \square, \iota(\mathbf{s}) = |\pm|, \iota(\mathbf{b}) = |\mathbf{0}|^1.$$

Given a unique identifier  $i \in \mathbb{N}$  for the unique symbol  $s_i$  and assuming that the type  $\tau(s_i)$  of the symbolic variable  $s_i$  is  $\mathbf{b}$  for boolean i.e.  $\tau(s_i) = \mathbf{b}$ , then  $\iota\tau(s_i) = |\mathbf{0}|^1 = \{0, 1\}$  is the interpretation  $\iota$  as a domain of the type  $\tau$  of the symbolic variable  $s_i$ . Indeed,  $|\mathbf{0}|^1$  is the domain of possible values for the boolean variable named as  $s_i$  when some value is assigned to it. Similarly,  $\iota\tau s^{-1}(i)$  denotes the domain of possible values for the symbolic variable uniquely identified by  $i$ , such domain depending on the type of  $s_i$ .

A Unique Symbols Provider (USP) is assumed to be implemented as a global function (or service) named  $!(\cdot)$  and such that  $!(n, t)$  with  $(n, t) \in \mathbb{N} \times \mathbb{T}$  returns an  $n$ -dimensional vector  $I \in \mathbb{I}^n$  of unique identifiers such that each related unique symbolic variable in the symbol vector  $s_I \in \mathbb{S}^n$  is of type  $t$  i.e.  $\forall i \in I, \tau(s_i) = t$ .

Notice that when the unique identifiers are integers i.e.  $\mathbb{I} = \mathbb{N}$ , a basic implementation of  $!(n, t)$  is “ $l = l + n$ ,

<sup>2</sup> here understood similarly to valuation in mathematical logic, e.g., as a (truth) value assignment to variables (in propositional logic).

<sup>3</sup> Since  $s$  is bijective,  $\forall s_i \in \mathbb{S}$  and  $\forall i \in \mathbb{I}$  are analog.

$\text{return}(h(t)\mathbf{1}_n + 2^{n_h}[l - n + 1, \dots, l])$ " where  $\mathbf{1}_n$  denotes a vector of  $n$  ones,  $l$  is a persistent counter initialized to 0 at startup, and  $h : \mathbb{T} \rightarrow \mathbb{N}$  assigns to each type  $t \in \mathbb{T}$  a unique integer encoded with at most  $n_h$  bits, which requires  $|\mathbb{T}| \leq 2^{n_h}$ . For example,  $\mathbb{T} = \{\emptyset, \mathbf{i}, \mathbf{s}, \mathbf{b}\}$  has a cardinality  $|\mathbb{T}| = 4$ . Then,  $n_h = 2$  and  $h(\mathbb{T}) = \{0, 1, 2, 3\}$  is a possible choice. Extensions include an overflow checking or an implementation (possibly distributed) as a service in a CPS (Cyber-Physical System) : see [17] for details.

### 3.2 s-functions

In order to transform and evaluate expressions based on (typed) symbols while preserving an explicit distinction between syntax and semantics, the notion of symbolic function or, shortly, s-function, is introduced. The aim is to disambiguate different interpretations of a function. Informally, let  $f$  be a function of  $s_1$  and  $s_2$  defined as  $f(s_1, s_2) = s_1 + s_2$  which is assumed to be a syntactically correct expression. Then, depending on the type of  $s_1$  and  $s_2$ , the possible values of  $s_1$  and  $s_2$  may differ as well as the concrete evaluation of the  $+$  operator e.g. sum of reals or sum of intervals, sum of scalars or sum of matrices, sum of crisp values or Minkowski sum of sets, concatenation of strings, etc. All the items in this enumeration are among the many possible interpretations of the same s-function  $f$  assigning the symbolic expression  $s_1 + s_2$  to the pair of parameters symbolized by  $(s_1, s_2)$ . Such interpretations may range from purely mathematical objects such as, e.g.,  $f : \mathbb{R}^2 \rightarrow \mathbb{R}, (s_1, s_2) \mapsto s_1 + s_2$ , to very concrete algorithmic implementations used to evaluate the image of some input parameter values. In the proposed symbolic framework, a distinction is explicitly made between s-function definitions (sfd), s-function interpretations (sfi), and s-function evaluations (sfe) based on a given sfi. Whereas sfd refers to syntax<sup>4</sup>, sfi and sfe refer to semantics.

Let  $f = \langle f \rangle_{s, \tau}$  denote an s-function of  $s_I$ ,  $I \subset \mathbb{I}$ , with symbols typed by  $\tau$ . Let  $\mathbb{F}(s_I)$  be the set of well-formed formulas/expressions/equations (wff) based on a language involving the (typed) symbols in  $s_I$ .

**Definition 6 (s-function: sfd/sfi/sfe) :**

- *s-function definition (sfd) :  $f = (I, F(s_I)) \in \mathbb{I} \times \mathbb{F}(s_I)$ .  $F(s_I)$  is a wff involving the (typed) symbolic variables in  $s_I$  which become bound in the formula: indeed,  $F(s_I)$  depends on  $s_I$ , at least from a syntactical viewpoint.*
- *s-function interpretation (sfi) : denoted as  $\iota f = \iota(f)$  or, possibly,  $[\iota f](.) = [\iota(f)](.)$  to emphasize the functional nature of an interpretation of the s-function  $f$ , an sfi of  $f$  has the ability to define and/or return output value(s) from input values corresponding to an interpretation/valuation of the symbols in  $s_I$ .*

<sup>4</sup> i.e. symbolically/formally/syntactically correct definitions

- *s-function evaluation (sfe) :  $[\iota f](\iota s_I)$  or, shortly<sup>5</sup>,  $\iota f(\iota s_I)$ , where  $\iota s_I$  (resp.  $\iota f$ ) stands for an interpretation/valuation of the symbolic vector  $s_I$  (resp. s-function  $f = (I, F(s_I))$ ). sfe refers to the result of a transformation process related to the semantic of symbolic terms.*

**Remark 7** Notice some analogy between the definition of sfd and the rule of abstraction in  $\lambda$ -calculus  $(\lambda x.M)$  [27,63,67]. Indeed, this rule also corresponds to the definition of an (anonymous) function based on a variable  $x$  and a wff  $M$  called  $\lambda$ -term, so that  $x$  becomes bound in the expression of  $M$ . That notion of being bound is essential to adequately handle dependencies. There are however at least two differences: firstly, the precise meaning of a wff is left open in the definition of sfd to allow for dealing with complex constructs more easily than with basic  $\lambda$ -calculus. Secondly, the symbolic variable(s) are referred to through unique identifiers which simplify some composition algorithms keeping trace of dependencies.

- i) In theory, an interpretation  $\iota f$  of the s-function  $f$  may refer to a classical mathematical function  $\iota f$  defined as  $\iota f : \iota s_I \rightarrow \iota \tilde{F}(\tau s_I), \iota s_I \mapsto \iota f(\iota s_I)$ , where the codomain is an interpretation of an output type inferred by  $\tilde{F}$  as a formal propagation of the input types  $\tau s_I$  through  $F(.)$ . The output type (resp. codomain) is possibly, but not necessarily, based on the basic symbol types in  $\mathbb{T}$  (resp.  $\mathbb{D}$ ).
- ii) In practice, an interpretation  $\iota f$  of the s-function  $f$  may be the execution of a syntactically correct algorithm related to the wff  $F(s_I)$ , and  $\iota s_I$  may be interpreted as the input value substituted for the symbolic input vector  $s_I$  in the code to perform the execution. By this way, a clear distinction is made between syntax  $(f, s_I)$  and semantics  $(\iota f, \iota s_I)$ , as is usually the case in mathematical logic. It is motivated by the need to truly formalize/catch non-trivial interactions between formal expressions, their mathematical interpretations, and related computations based on algorithms manipulating dedicated data structures.

**Remark 8** i) The interpretation of a formula like  $F(.)$  to build  $[\iota f](.)$  may involve, or not, a (co)recursive evaluation of the operators in its structure, so that a non-strict/lazy/delayed evaluation is possible. Non-strict refers to an evaluation strategy where the arguments of a function are not immediately evaluated, as in functional programming languages. Lazy-evaluation, also named call-by-need, has connections with graph reduction, and makes it possible to work with potentially infinite data structures, which looks appealing to further deal with hybrid systems and model reduction.

ii) Even if not mandatory, an s-function evaluation may

<sup>5</sup> A priori,  $\iota f(\iota s_I)$  may refer to either  $\iota(f)(\iota s_I)$  or  $\iota(f(\iota s_I))$  which might be ambiguous.

return an *s*-function definition e.g.  $[\iota f](\iota s_I) = (J, G(s_J))$  where  $J$  identifies the symbols in the *sfd* resulting from the evaluation (with possibly  $I \cap J \neq \emptyset$ ),  $G(s_J)$  is a wff, and global dependencies can be preserved through *s*. Taking the identity for *f* shows that any symbol may be interpreted as a function, as in  $\lambda$ -calculus and a purely functional paradigm. Since random variables are nothing else but functions from a set of outcomes to a set of possible values, the proposed framework of image-sets with typed symbols is fully open to stochastic descriptions.

### 3.3 Image-sets

The (classical) notions of *imset* and *inclusion function* as defined in the preliminaries (section 2) are extended to the proposed symbolic framework through the definitions of *image-sets* and *inclusion s-functions*:

**Definition 9 (Image-set)** The image-set  $\langle f \rangle_{s, \tau, \iota}$  of the *s*-function  $f = \langle f \rangle_{s, \tau} = (I, F(s_I))$ , under an interpretation  $\iota f$  of *f* and  $\iota \tau$  of the typing function  $\tau(\cdot)$ , is the *imset* of the domain  $\iota \tau s_I$  by  $\iota f$ :

$$\langle f \rangle_{s, \tau, \iota} = \{\iota f(\sigma) \mid \sigma \in \iota \tau s_I\} = \iota f(\iota \tau s_I),$$

where  $\sigma$  refers to a generic interpretation/value  $\iota s_I$  of  $s_I$  and  $\iota f(\sigma)$  is a shorthand notation for  $[\iota(f)](\sigma)$ .

**Remark 10** The domain  $\iota \tau s_I$  is a set related to the types of the symbols in  $s_I$ .

**Definition 11 (Inclusion s-function)** The *s*-function  $g = (J, G(s_J))$  is an inclusion *s*-function for  $f = (I, F(s_I))$  under given interpretations  $\iota_F$ ,  $\iota_G$ ,  $\iota \tau$  of *f*, *g*, and the symbol typing function  $\tau(\cdot)$ , if  $\iota g$  is an inclusion function for  $\iota f$  defined on the domain  $\iota \tau s_I$ . Notably,  $\iota f(\cdot)$  and  $\iota g(\cdot)$  being shorthands for  $[\iota(f)](\cdot)$  and  $[\iota(g)](\cdot)$ ,

$$\forall \Sigma \in \llbracket \iota \tau s_I \rrbracket, \{\iota f(\sigma) \mid \sigma \in \Sigma\} = \iota f(\Sigma) \subset \iota g(\Sigma). \quad (1)$$

**Corollary 12** From the definition 2 and its corollary 4,  $\iota f(\Sigma)$  being the *imset* of  $\Sigma$  by  $\iota f$ , and  $\iota g(\iota \tau s_I)$  being the image of  $\iota \tau s_I$  by  $\iota g$ , it comes:

$$\forall \Sigma \in \llbracket \iota \tau s_I \rrbracket, \iota f(\Sigma) \subset \iota g(\iota \tau s_I). \quad (2)$$

**Definition 13 (Reduction)** A reduction is an operator  $\downarrow_q$  transforming an *s*-function  $f = (I, F(s_I))$  into an *s*-function  $\bar{f} = \downarrow_q f = (\bar{I}, \bar{F}(s_{\bar{I}}))$  such that  $\bar{f}$  is an inclusion *s*-function for *f* depending on at most  $q$  generator symbols:  $\text{card}(\bar{I}) \leq q \in \mathbb{N}$  and  $\text{card}(\cdot)$  gives the cardinal. Remark:  $\bar{I} \cap I \neq \emptyset$  is not mandatory but often useful to limit the inclusion conservatism while controlling the complexity of  $\bar{f}$  through its input dimension.

Notice that the validity of the inclusion in (1) now depends on explicitly given interpretations of *f*, *g*,  $\tau(\cdot)$ . In the following, the interpretation  $\iota f$  of *f* in the definition 11 will be always as a ‘mathematical function’ as

indicated by the subscript *m* in  $\iota f = \iota_m f$ . It may refer to some basic model of a system. By contrast, at least two possible interpretations of *g* may coexist:  
*i*)  $\iota_{\bar{m}} : \text{interpretation as a 'set-valued' }^6 \text{ mathematical function'}$ . Then,  $\iota g = \iota_{\bar{m}} g = [\iota_{\bar{m}}(g)](\cdot)$  refers to some set-valued model that may be qualified as robust if it preserves inclusion. (1) becomes:

$$\forall \Sigma \in \llbracket \iota \tau s_I \rrbracket, \{\iota_m f(\sigma) \mid \sigma \in \Sigma\} \subset \iota_{\bar{m}} g(\Sigma).$$

This inclusion refers to a *first* kind of potential conservatism, the one possibly induced by rewriting mathematical functions while preserving inclusion e.g. simplifications, model reduction, etc.

*ii*)  $\iota_a : \text{interpretation as the 'execution of an inclusion algorithm' used as a practical implementation'}$ . Then,  $\iota_a g(\cdot) = [\iota_a(g)](\cdot)$  refers to how some concrete abstractions of image domains<sup>7</sup> can be obtained so as to further manipulate them as efficiently as possible from a computational perspective, while preserving an inclusion property. Applying the definition 11 with  $f = g$  (same symbolic expressions) under the interpretation  $\iota_m$  for *f* and  $\iota_a$  for *g* particularizes (1) as:

$$\forall \Sigma \in \llbracket \iota \tau s_I \rrbracket, \{\iota_m f(\sigma) \mid \sigma \in \Sigma\} \subset \iota_a g(\Sigma).$$

Since  $\iota_m f$  is interpreted as a mathematical function and  $f = g$ , the *imset* (definition 1) of  $\Sigma$  by  $\iota_m g$  and the corollary 4 with  $\mathbb{X} = \iota \tau s_I$  give:

$$\forall \Sigma \in \llbracket \iota \tau s_I \rrbracket, \iota_m g(\Sigma) \subset \iota_a g(\iota \tau s_I).$$

This inclusion refers to a *second* kind of potential conservatism, the one induced by the practical need to compute over finite abstractions based on domains rather than over all the possible concrete individual crisp values and subsets (infinite cardinal on continuous domains, highly combinatorial on discrete domains). Bisection/splitting can be used to struggle against that second kind of conservatism, but often at the price of an exponential complexity.

To summarize, two kinds of conservatism induced by inclusion preservation have been distinguished :

- i*) the one related to some problem (re)formulation and modeling through mathematical functions,
- ii*) the one related to practical algorithmic computations over domains.

Each kind of conservatism has been related to particular interpretations of symbolic well-formed formulas.

**Example 14**  $\mathbb{I} = \mathbb{N}$ ,  $\mathbb{S} = \{s_i = s(i), i \in \mathbb{I}\}$  where *s* is a (global) function.  $I = [1; 2] \subset \mathbb{I}$ ,  $s_I = [s_1; s_2]$  is a vector of symbols of type (unit) interval:  $\tau(s_I) = [\mathbf{i}; \mathbf{i}]$ , leading to the domain  $\iota \tau s_I = \square^2 \subset \mathbb{R}^2$ . Let *f* be the *s*-function  $f = (I, F(s_I))$  based on the wff  $F(s_I) = [1 + s_1 + s_2^3 - 0.8s_1; s_1]$  where  $+$ ,  $-$ ,  $[;]$  are operator symbols for plus, minus, vertical concatenation, respectively. *f* can be interpreted as a (punctual) mathematical function e.g.

<sup>6</sup> Whereas  $\iota_m g : \iota \tau s_J \rightarrow \iota \tilde{G}(\tau s_J)$ ,  $\sigma \mapsto \iota_m g(\sigma)$  may not be set-valued,  $\iota_{\bar{m}} g : \llbracket \iota \tau s_I \rrbracket \rightarrow \llbracket \iota \tilde{F}(\tau s_I) \rrbracket$ ,  $\Sigma \mapsto \iota_{\bar{m}} g(\Sigma)$  necessarily is.

<sup>7</sup> The need for abstraction is motivated by the nature of such image domains: possibly infinite in continuous cases and/or highly combinatorial in discrete cases.

$\iota_m f : \square^2 \rightarrow \mathbb{R}^2$ ,  $[v_1; v_2] \mapsto [1 + v_1 + v_2^3 - 0.8v_1; v_1]$  where  $\mathbb{R}$  refers to the real field equipped with usual operations. Let  $g \neq f$  i.e.  $g$  and  $f$  have distinct symbolic expressions:  $J = [1; 3]$ ,  $\tau(s_J) = [\mathbf{i}; \mathbf{i}]$ , and  $G(s_J) = [1 + 0.2s_1 + s_3; s_1]$ . One possible interpretation  $\iota_m$  of  $g$  as a set-valued mathematical function is  $\iota_m g : \llbracket \square^2 \rrbracket \rightarrow \llbracket \mathbb{R}^2 \rrbracket$ ,  $V \mapsto \{[1 + 0.2v_1 + v_3; v_1] \mid [v_1; v_2] \in V \wedge v_3 \in \square\}$ , where  $\llbracket \mathcal{D} \rrbracket$  denotes a set of subsets of  $\mathcal{D}$ . Another interpretation  $\iota_a$  of  $g$  as the execution of an inclusion algorithm may be based on the so-called natural interval extension giving  $\iota_a g([v_1; v_2]) = [1 \oplus 0.2v_1 \oplus \square; v_1]$ , where  $\oplus$  and  $\ominus$  refer to interval arithmetic operators for plus and minus. Then, i) Case of  $\iota_m g$ .  $g$  is an inclusion s-function for  $f$  under the interpretations  $\iota_m g$ ,  $\iota_m f$ ,  $\iota\tau$  since  $\forall \Sigma \in \llbracket \square^2 \rrbracket$ ,  $\iota_m f(\Sigma) = \{[1 + \sigma_1 + \sigma_2^3 - 0.8\sigma_1; \sigma_1] \mid \sigma \in \Sigma\} \subset \iota_m g(\Sigma) = \{[1 + 0.2\sigma_1 + \sigma_3; \sigma_1] \mid \sigma_1 \in \Sigma_1 \wedge \sigma_3 \in \square\}$ , where  $\Sigma_1$  is the projection of  $\Sigma$  along the 1st dimension ( $\{1\} = I \cap J$ ). Notice that when  $\Sigma \subset \square^2$  is a 2D interval, then  $\iota_m g(\Sigma)$  is an enclosing zonotope for the imset of  $\Sigma$  by  $\iota_m f$ . ii) Case of  $\iota_a g$ .  $g$  is an inclusion s-function for  $f$  under the interpretations  $\iota_a g$ ,  $\iota_m f$ ,  $\iota\tau$  since  $\forall \Sigma \in \llbracket \square^2 \rrbracket$ ,  $\iota_m f(\Sigma) = \{[1 + \sigma_1 + \sigma_2^3 - 0.8\sigma_1; \sigma_1] \mid \sigma \in \Sigma\} \subset \iota_a g(\Sigma) = [1 \oplus 0.2\Sigma_1 \oplus \square; \Sigma_1] \subset [1 \oplus 0.2\square \oplus \square; \square] = [1 \pm 1.2; 0 \pm 1] \subset \mathbb{R}^2$ , where the second inclusion comes from the corollary 4, and  $c \pm r$  denotes the interval  $[c - r, c + r]$ . A natural interval extension  $\iota_a$  directly applied to  $f$  would give the interval  $1 \pm 2.8$  instead of  $1 \pm 1.2$  for the first component: the improved accuracy obtained with  $f \neq g$  has been obtained by rewriting the initial wff  $F(s_I)$  of  $f$  as  $G(s_J)$ . The later exhibits a reduced number of symbol multi-occurrences, while the principle underlying the algorithmic interpretation  $\iota_a$  remains identical.

The proposed framework is exemplified with, but not at all restricted to, interval arithmetic and related natural extensions. It is indeed much more general.

The example 14 outlines and motivates the strategy further developed to reduce conservatism in a generic way: i) Rewrite the symbolic expression (wff)  $F(s_I)$  of  $f$  as  $G(s_J)$  in an inclusion s-function  $g$ , by elimination of symbol multi-occurrences and, possibly, by reducing the number of symbols in  $s_J$  compared to  $s_I$ . The trade-off between enclosure accuracy and computational complexity requires that such a reduction preserves the more important symbols/dependencies i.e. the ones which significantly contribute to shaping the graph of the mathematical function symbolized by the s-function  $f$ . ii) Delay as much as possible (i.e. lazy-evaluation/call-by-need) the use of interval computations  $\iota_a$  because, once applied, the dependencies on the individual elements in the domain  $\iota\tau s_I$  may be lost, especially if a natural interval extension is used.

Moreover, the framework of image-sets with typed symbols proposed in this work is well-suited by design to naturally handle mixed, continuous and discrete sets:

### Definition 15 (Mixed, continuous, discrete)

Let  $\{\mathbb{T}_c, \mathbb{T}_d, \mathbb{T}_o\}$  be a partition of the types in  $\mathbb{T}$

into continuous ( $\mathbb{T}_c$ ), discrete ( $\mathbb{T}_d$ ), and other ones ( $\mathbb{T}_o$ ). Let  $I \subset \mathbb{I}$  and  $T_I = \cup_{i \in I} \{\tau s_i\}$ . The symbolic vector  $s_I$  is mixed (resp. continuous, discrete) if  $(T_I \cap \mathbb{T}_c \neq \emptyset) \wedge (T_I \cap \mathbb{T}_d \neq \emptyset)$  (resp.  $T_I \subset \mathbb{T}_c, T_I \subset \mathbb{T}_d$ ). By extension, any formula  $F(s_I)$ , s-function, image-set, (s-)zonotope, (s-)polynotope, etc can be qualified as mixed, continuous<sup>8</sup> or discrete accordingly.

## 4 Generality of the framework: Illustration

**Assumption 16** The symbol types  $\mathbb{T} = \{\emptyset, \mathbf{i}, \mathbf{s}, \mathbf{b}\}$ , the domains  $\mathbb{D} = \{\emptyset, \square, \llbracket \cdot \rrbracket, \llbracket \cdot \rrbracket_0^1\}$  and the related interpretation function  $\iota_{\mathbb{T}}$  previously considered in the example 5 are considered by default in the following with  $\mathbb{T}_c = \{\mathbf{i}\}$ ,  $\mathbb{T}_d = \{\mathbf{s}, \mathbf{b}\}$ ,  $\mathbb{T}_o = \{\emptyset\}$ . By default, basic scalar values are assumed to be interpreted in the real field  $\mathbb{R}$  equipped with the usual sum and product operators.

**Corollary 17** In an entirely continuous case, following the assumption 16, all the symbols in  $s_I$  are of type (unit) interval:  $\forall i \in I, \tau s_i = \mathbf{i}$ , that is,  $\forall i \in I, \iota\tau s_i = \square = [-1; +1]$ . As a result, for any vector  $I$  of  $n$  unique identifiers only referring to continuous symbols, any single-valued interpretation<sup>9</sup>  $\iota s_I$  of the symbolic vector  $s_I$  belongs to the unit interval  $\square^n$ :  $\forall \iota_{\mathbb{S}}, \iota s_I \in [-1; +1]^n$ .

### 4.1 Affine s-functions and zonotopes

**Definition 18 (Affine/linear wff)** The wff  $F(s_I)$  is affine in  $s_I$  if it can be written as  $c + R s_I$  where the vector  $c$  and the matrix  $R$  do not depend on the symbolic variables in  $s_I$ . In particular, it is linear when  $c$  is null or can be omitted i.e.  $F(s_I) = R s_I$ . Shortly,

$$\text{Affine wff: } F(s_I) = c + R s_I.$$

**Definition 19 (s-zonotope)** A symbolic zonotope (s-zonotope) is an s-function  $f = \langle f \rangle_{s, \tau} = (I, F(s_I))$  such that the wff  $F(\cdot)$  is affine in the symbolic variables in  $s_I$ .

**Definition 20 (e-zonotope)** The e-zonotope related to the s-zonotope  $\langle f \rangle_{s, \tau}$  is the image-set  $\langle f \rangle_{s, \tau, \iota}$  of  $f = \langle f \rangle_{s, \tau}$  under an affine interpretation  $\iota f$  of  $f$ . An e-zonotope is thus a set-valued evaluation (semantics) related to a given s-zonotope (syntax).

One possible data structure to store a symbolic zonotope is  $(c, R, I)$ . The related s-function defined by a wff denoted  $\langle c, R, I \rangle_{s, \tau}$  is  $f = (I, c + R s_I)$ , and the related e-zonotope is in (4):

$$\langle c, R, I \rangle_{s, \tau} = c + R s_I \quad (\text{syntax}) \quad (3)$$

$$\langle c, R, I \rangle_{s, \tau, \iota} = \{c + R\sigma \mid \sigma \in \iota\tau s_I\} \quad (\text{semantics}) \quad (4)$$

<sup>8</sup> Regarding functions, continuous refers here to a property of the input domain and not to continuity as in analysis.

<sup>9</sup> as long as it is consistent with the type (unit) interval.

The main differences with classical zonotopes defined as  $\langle c, R \rangle = \{c + Rs \mid s \in [-1, +1]^n\}$  are twofold:

Firstly, the interplay between syntax and semantics is not caught by the classical definition, whereas it plays a key role in the management of the so-called dependency problem. For example, assuming an entirely continuous case as in corollary 17 i.e. all the symbols  $s_i$  are of type (unit) interval, let consider the sum  $S$  (resp. Minkowski sum  $S_\iota$ ) of the s-zonotopes<sup>10</sup>  $\langle 0, 1, 1 \rangle_{s, \tau}$  and  $\langle 0, -1, 1 \rangle_{s, \tau}$  (resp.  $\langle 0, 1, 1 \rangle_{s, \tau, \iota}$  and  $\langle 0, -1, 1 \rangle_{s, \tau, \iota}$ ). Then,  $S = 0 + s_1 - s_1 = 0$  (resp.  $S_\iota = \square + \square = 2\square = [-2, +2]$ ), and the set-valued interpretation  $\iota S = \{0\}$  of  $S$  is much less conservative than  $S_\iota = [-2, +2]$  while preserving the inclusion property under the considered semantics. Indeed, some uncertainty cancellation has been made possible by formal/symbolic transformations respecting operators syntactic rules, whereas this is no more possible through the Minkowski sum following a set-valued evaluation. One strategy to improve accuracy thus consists in delaying such set-valued evaluations. Moreover, whereas  $\forall i \in \mathbb{I}, \langle 0, 1, i \rangle_{s, \tau, \iota} = \langle 0, 1 \rangle = [-1; +1], \langle 0, 1, i \rangle_{s, \tau} = s_i$  is distinct from  $\langle 0, 1, j \rangle_{s, \tau} = s_j$  as long as  $i \neq j$ .

From a computational perspective, Matrices with Labelled Columns (MLC) featuring a column-wise sparsity as first introduced in [17] lead to efficient implementations of s-zonotope operators such as sum, linear image, interval/box hull, etc. The reader is referred to [17] for a detailed description, especially in the sections 4 “Matrices with Labeled Columns (MLC)” and 6 “Symbolic zonotopes”. Notice that the definition of symbolic zonotopes in [17] only considers one type of symbols interpreted as random variables with support in the unit interval  $[-1, +1]$ . This outlines how the general framework described in section 3 can also be used in a stochastic paradigm: Indeed, it suffices to consider other types of symbols interpreted as random variables (which are themselves functions, so emphasizing the relevance of cross-connections with functional paradigms). In order to give a flavor about MLC, an informal definition and a sum example are provided. An MLC  $M^{|I|}$  is a pair  $(M, I^T)$  where  $M$  is an  $n \times p$  matrix and  $I \in \mathbb{I}^p$  is a vector such that each scalar  $I_j$  for  $j = 1, \dots, p$ , uniquely identifies the  $j$ th column  $M_{:,j}$  of  $M$ . Shortly, the column of  $M^{|I|}$  labeled as  $I_j$  refers to  $M_{:,j}$ . An example illustrating the sum of two MLC,  $M^{|I|} + N^{|J|} = P^{|K|}$  is:

$$\begin{bmatrix} 2 & 1 & 5 \\ 1 & 0 & 1 \\ 0 & 1 & 1 \end{bmatrix} + \begin{bmatrix} 3 & 5 & 2 & 8 \\ 2 & 0 & 4 & 6 \\ 0 & 3 & 5 & 7 \end{bmatrix} = \begin{bmatrix} 1 & 2 & 5 & 3 & 8 \\ 0 & 5 & 1 & 2 & 6 \\ 1 & 5 & 4 & 0 & 7 \end{bmatrix}. \quad (5)$$

<sup>10</sup> here, the s-function is identified to the wff used to define it.

$$\begin{bmatrix} 0 & 5 & 1 & 2 & 6 \\ 1 & 5 & 4 & 0 & 7 \end{bmatrix} \begin{bmatrix} s_1 \\ s_2 \\ s_5 \\ s_3 \\ s_8 \end{bmatrix} = \begin{bmatrix} 1 & 0 & 1 \\ 0 & 1 & 1 \end{bmatrix} \begin{bmatrix} s_2 \\ s_1 \\ s_5 \end{bmatrix} + \begin{bmatrix} 2 & 0 & 4 & 6 \\ 0 & 3 & 5 & 7 \end{bmatrix} \begin{bmatrix} s_3 \\ s_5 \\ s_2 \\ s_8 \end{bmatrix} \quad (6)$$

As shown in (5), an equal number of columns/generators of the operands is not mandatory, and the labels are reported on the first lines (e.g.  $I^T = [2, 1, 5]$ ). (6) illustrates the column-wise (not row-wise) sparsity granted by MLC operators, and that the sum of two MLC gives the exact sum of two centered s-zonotopes since  $\langle 0, P, K \rangle_{s, \tau} = \langle 0, M, I \rangle_{s, \tau} + \langle 0, N, J \rangle_{s, \tau}$ . Indeed,  $M^{|I|} + N^{|J|} = P^{|K|} \Rightarrow M s_I + N s_J = P s_K$ .  $K \subset I \cup J$  results from merging the unique identifiers in  $I$  and  $J$  while removing those possibly related to null generators. The vertical concatenation  $[M^{|I|}; N^{|J|}] = [M^{|I|}; 0] + [0; N^{|J|}]$  also illustrates close links between sum and concatenation of MLC.

Secondly, another main difference with classical zonotopes is the introduction of symbol typing. This makes it possible to combine several kinds of interpretations. Following the assumption 16, this paper mainly focuses on mixed, continuous and discrete values in a set-membership paradigm, though the framework described in section 3 is more general. For example, let consider five symbols  $s_i, i = 1, \dots, 5$ , such that  $s_1, s_2, s_3$  are of type **s** (signed) i.e.  $s_1, s_2, s_3$  take their values in the discrete set  $\{-1, +1\}$ , and  $s_4, s_5$  are of type **i** (interval) i.e.  $s_4, s_5$  take their values in the unit interval  $[-1, +1] \subset \mathbb{R}$ . Let  $I_1 = [1, 2, 3]$  and  $I_2 = [4, 5]$  be vectors of unique identifiers gathering symbols according to their type: Following the definition 15,  $s_{I_1}$  is discrete,  $s_{I_2}$  is continuous, and  $s_I$  with  $I = [I_1; I_2]$  is mixed. Let  $R_1 = [3, 3, -3; 6, -5, 9], R_2 = [4, 2; 2, -4]$  and  $R = [R_1, R_2]$ . Then, the (discrete) e-zonotope  $\langle 0, R_1, I_1 \rangle_{s, \tau, \iota}$  is a set of eight<sup>11</sup> points which are the linear images by  $R_1$  of the vertices of a 3D unit hypercube since  $\iota s_{I_1} \in \iota \tau s_{I_1} = \{-1, +1\}^3$ . The (continuous) e-zonotope  $\langle 0, R_2, I_2 \rangle_{s, \tau, \iota}$  is the classical zonotope  $\langle 0, R_2 \rangle$  i.e. the linear image by  $R_2$  of a 2D unit hypercube since  $\iota s_{I_2} \in \iota \tau s_{I_2} = [-1, +1]^2$ . More interestingly, the (mixed) e-zonotope  $\langle 0, R, I \rangle_{s, \tau, \iota}$  is the linear image by  $R = [R_1, R_2]$  of  $\iota \tau s_I = \{[-1, +1]^3; [-1; +1]^2\}$ . It is also the Minkowski sum of the (discrete) e-zonotope  $\langle 0, R_1, I_1 \rangle_{s, \tau, \iota}$  and the (continuous) e-zonotope  $\langle 0, R_2, I_2 \rangle_{s, \tau, \iota}$ . The resulting set is neither convex nor connected, as shown in Fig. 1, where the dashed line is the border of the classical (continuous) zonotope  $\langle 0, R \rangle$ . This example illustrates that mixed zonotopes can provide a very compact representation (Fig.1:  $R \in \mathbb{R}^{2 \times 5}$  and 5 bits encoding the symbol types) for the union of a same<sup>12</sup> (continuous) zonotopic shape centered on

<sup>11</sup> It could be less if some image points are identical.

<sup>12</sup> Relaxing this constraint is among the motivations to the

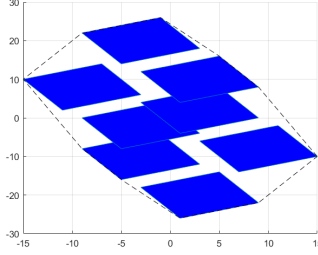


Fig. 1. Example of mixed e-zonotope  $\langle 0, R, I \rangle_{s,\tau,\iota}$ .

each point of a discrete set possibly containing a high number of configurations (Fig. 1:  $2^3 = 8 =$  cardinal of  $\{-1, +1\}^3$ ).

#### 4.2 Mixed encoding

The notion of *mixed encoding* is introduced in the same spirit as the example illustrated in Fig. 1. It also provides a framework for a hierarchical modeling of dependencies making it possible to tune the granularity level of the description. Notation: Let  $\square_i$  (resp.  $|\pm|_i$ ,  $|_0^1|_i$ ) denote the symbol  $s_i$  provided it is of type interval (resp. signed, boolean) i.e.  $\tau s_i = i$  (resp. **s**, **b**). Under the assumption 16, a compact notation for typed symbols is so obtained, each being uniquely identified by  $i$ . Also, let  $\rho(0) = 1$ ,  $\rho(n+1) = \frac{1}{2}[1, \rho(n)]$  for  $n \in \mathbb{N}$ . Then,  $\forall n$ ,  $\rho(n) = [(\frac{1}{2})^1, \dots, (\frac{1}{2})^n, (\frac{1}{2})^n] \in \mathbb{R}^{1 \times (n+1)}$ . By induction, the row sum of  $\rho(n)$  is 1.

**Definition 21 (Mixed encoding of basic intervals)** The *s*-zonotope  $Z_s^n(I)$  is an  $n$ -level signed-interval mixed encoding of the unit interval  $[-1, +1]$  if

$Z_s^n(I) = \langle 0, \rho(n), I \rangle_{s,\tau} = (\sum_{j=1}^n (\frac{1}{2})^j \#|I_j|) + (\frac{1}{2})^n \square_{I_{n+1}}$ .  
The *s*-zonotope  $Z_b^n(I)$  is an  $n$ -level boolean-interval mixed encoding of the interval  $[0, 1]$  if

$$Z_b^n(I) = \langle 0, \rho(n), I \rangle_{s,\tau} = (\sum_{j=1}^n (\frac{1}{2})^j |_0^1|I_j|) + (\frac{1}{2})^n \square_{I_{n+1}}.$$

**Corollary 22 (Mixed encoding of intervals)** Let  $Z_s^n(I)$  be a mixed encoding of  $[-1, +1]$ . Then,  $c + rZ_s^n(I)$  is a mixed encoding of  $c \pm r = [c - r, c + r]$ .

Let  $Z_b^n(I)$  be a mixed encoding of  $[0, 1]$ . Then,  $a + (b - a)Z_b^n(I)$  is a mixed encoding of  $[a, b]$ .

**Corollary 23 (Related e-zonotopes)** Following the definition 21, the *e*-zonotope related to the *s*-zonotope  $Z_s^n(I)$  (resp.  $Z_b^n(I)$ ) is  $[-1, +1]$  (resp.  $[0, 1]$ ). Conversely, there is no unique mixed encoding for a given interval. The *e*-zonotope  $(c + rZ_s^n(I))_\iota$  related to the *s*-zonotope  $c + rZ_s^n(I)$  satisfies  $(c + rZ_s^n(I))_\iota \subseteq (c \pm r)$  (interval hull). The equality holds in the scalar case or for  $r = 0$ .

The surjective nature of mixed encoding gives freedom degrees to model dependencies in a hierarchical way. The

polynomial extension in §4.3.

discrete parts feature close analogies with the usual binary encoding of integers. Moreover, the coverage of continuous domains is achieved through remainder terms. The width of the set-valued interpretation of these terms is related to the granularity of the mixed-encoding. It can be refined or reduced by adapting the level value  $n$ . Since affine *s*-functions and zonotopes essentially provide operators managing affine dependencies only, and since this yields some restrictions on the possible uses of mixed encoding (among others: see, e.g., footnote 12), an extension to polynomial dependencies is considered.

#### 4.3 Polynomial *s*-functions and polynotopes

Let  $(\boxplus, \boxtimes)$  denote a generic matrix product:  $M(\boxplus, \boxtimes)N = \boxplus_{j=1}^p (M_{ij} \boxtimes N_{jk})$ , where  $p$  both refers to the number of columns of  $M$  and the number of rows of  $N$ . For example,  $MN = M(+, \cdot)N$  is the classical matrix product.  $+, \cdot, \hat{\cdot}$  respectively denote sum, product, power.

**Definition 24 (Monomial matrix notation)** The monomial matrix  $\theta^E$  is  $(\theta^T(\cdot, \hat{\cdot})E)^T$ , where  $\theta$  (resp.  $E$ ) is a so-called variable matrix (resp. exponent matrix) of dimension compatible with the generic matrix product  $(\cdot, \hat{\cdot})$ . The operator  $^T$  refers to transposition.

Examples: Taking  $\theta = [s_1; s_2]$  and  $E = [1, 0, 2; 0, 3, 4]$  yields  $\theta^E = [s_1; s_2^3; s_1^2 s_2^4]$ .  $\theta^I = \theta$  with  $I =$  identity.

**Definition 25 (Polynomial wff)** The wff  $F(s_I)$  is polynomial in  $s_I$  if it can be written as  $c + Rs_I^E$  where the vector  $c$  and the matrices  $R$  and  $E$  do not depend on the symbolic variables in  $s_I$ . Shortly,

$$\text{Polynomial wff: } F(s_I) = c + Rs_I^E.$$

Then,  $c$ ,  $R$ ,  $s_I$ ,  $E$ ,  $s_I^E$  are respectively the so-called constant vector, coefficient/generator matrix, symbol(ic variable) vector, exponent matrix, monomial vector.

**Definition 26 (s-polynotope)** A symbolic polynotope (*s*-polynotope) is an *s*-function  $f = \langle f \rangle_{s,\tau} = (I, F(s_I))$  such that the wff  $F(\cdot)$  is polynomial in the symbolic variables in  $s_I$ .

**Definition 27 (e-polynotope)** The *e*-polynotope related to the *s*-polynotope  $\langle f \rangle_{s,\tau}$  is the image-set  $\langle f \rangle_{s,\tau,\iota}$  of  $f = \langle f \rangle_{s,\tau}$  under a polynomial interpretation  $\iota$  of  $f$ . An *e*-polynotope is thus a set-valued evaluation (semantics) related to a given *s*-polynotope (syntax).

The name polynotope introduced in this work originates from a contraction of polynomial and zonotope. Following [31], it is also willingly close to polytope. So, *polynotope* gathers, at least partially, the Greek roots of polynomial (from *polus*:numerous and *nomos*:division) and polytope (from *polus* and *topos*:location).

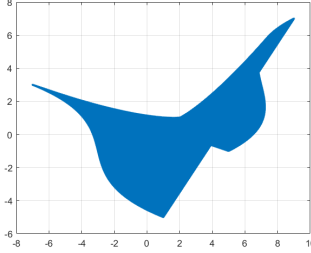


Fig. 2. Example of continuous e-polynotope  $\langle c, R, I, E \rangle_{s, \tau, \iota}$ .

One possible data structure to store a symbolic polynotope is  $(c, R, I, E)$ . The related s-function defined by a wff denoted  $\langle c, R, I, E \rangle_{s, \tau}$  is  $f = (I, c + Rs_I^E)$ , and the related e-polynotope is in (8):

$$\langle c, R, I, E \rangle_{s, \tau} = c + Rs_I^E \quad (\text{syntax}) \quad (7)$$

$$\langle c, R, I, E \rangle_{s, \tau, \iota} = \{c + R\sigma^E \mid \sigma \in \iota\tau s_I\} \quad (\text{semantics}) \quad (8)$$

Polynotopes as in (7)-(8) generalize zonotopes as in (3)-(4). Indeed, zonotopes are obtained for  $E = \mathcal{I}$  (identity matrix) which is highly sparse and can thus be stored very efficiently. Using a sparse  $E$  with integer entries in  $\mathbb{N}$  leads to a data structure similar to sparse polynomial zonotopes (spz) in [32], where no typing of symbols is considered (continuous case only). The sparsity of  $E$  extends the column-wise sparsity of MLC to polynomial (rather than affine) dependencies with a compact description of monomials featuring (almost) no restriction on the highest degree. The example (9)-(10) shows how the s-polynotope related to (10) can be compactly encoded using  $(c, R, I, E)$  as in (9). See also Fig. 2.

$$\left[ \begin{array}{c|c} I & E \\ \hline c & R \end{array} \right] = \left[ \begin{array}{c|ccc} 1 & 1 & 0 & 1 \\ 8 & 0 & 3 & 1 \\ 2 & 5 & 3 & -1 \\ 1 & 2 & 0 & 4 \end{array} \right], \quad (9)$$

$$\left[ \begin{array}{c} s_1 \\ s_8 \end{array} \right] \mapsto \left[ \begin{array}{c} 2 + 5s_1 + 3s_8^3 - s_1s_8 \\ 1 + 2s_1 + 4s_1s_8 \end{array} \right]. \quad (10)$$

The implementation of continuous polynotopes operations used in this work is close to the one described in [32] for spz. In particular, each time monomial redundancies might occur, they are removed by summing the related generators: all the columns of  $E$  remain distinct. The main differences are:

- 1) The case of independent generators is not treated separately i.e. all the generators are possibly dependent (provided they share some common symbol),
- 2) The implementation of a symbolic addition is considered and optimized by taking into account the fact that monomials/generators involving at least one own variable from an operand can be simply copied in the result

since no similar monomial exists in the other operand,  
3) A vertical concatenation extends the one of MLC,  
4) An element-wise product is used as a special case of quadratic map and the reduction extends the one in [17].

Our implementation of polynotopes also supports discrete and mixed operations through symbol typing as described in section 3 and assumption 16. Compared to a strictly continuous case as in [32], the main difference is the introduction of rewriting rules taking the specific nature of signed and boolean symbols into account. Related substitutions ( $\rightarrow$ ) are implemented very efficiently using the  $(c, R, I, E)$  attributes with sparse  $E$ , e.g.

$$(|\pm|_i)^n \rightarrow (|\pm|_i)^{\text{mod}(n,2)}, \quad (11)$$

$$(|^1_0|_i)^n \rightarrow (|^1_0|_i)^{\text{max}(n,1)}. \quad (12)$$

**Definition 28 (Rewriting rules and inclusion)** A rewriting rule is inclusion preserving if:

$$(\langle f \rangle_{s, \tau} \rightarrow \langle g \rangle_{s, \tau}) \Rightarrow (\langle f \rangle_{s, \tau, \iota} \subseteq \langle g \rangle_{s, \tau, \iota}).$$

It is inclusion neutral if:

$$(\langle f \rangle_{s, \tau} \rightarrow \langle g \rangle_{s, \tau}) \Rightarrow (\langle f \rangle_{s, \tau, \iota} = \langle g \rangle_{s, \tau, \iota}).$$

**Proposition 29** The rewriting rules in (11) and (12) are inclusion neutral under the assumption 16.

Notice the syntactical (resp. semantic) nature of the premises (resp. conclusions) of the implications ( $\Rightarrow$ ) in the definition 28. To give insight into the proposition 29, let  $x$  be a possible value of any signed symbol:  $x \in \{-1, +1\} \subset \mathbb{R}$ . Thus,  $(x+1)(x-1) = 0$  i.e.  $x^2 = 1$ . By induction,  $x^n = x$  for odd  $n$ ,  $x^n = 1$  for even  $n$ , that is  $x^n = x^{\text{mod}(n,2)}$  which shows the inclusion neutrality of (11). Similarly, let  $x$  be a possible value of any boolean symbol:  $x \in \{0, 1\} \subset \mathbb{R}$ . Thus,  $(x-0)(x-1) = 0$  i.e.  $x^2 = x$ . By induction,  $x^n = x$  if  $n > 1$ ,  $x^n = 1$  if  $n = 0$ , that is  $x^n = x^{\text{max}(n,1)}$  which shows the inclusion neutrality of (12).

The rewriting rules (11)-(12) apply for operations modifying the monomial degrees like product; the number of distinct monomials induced by discrete operations is drastically reduced compared to continuous ones, since the exponent in the right term of (11)-(12) is either 0 or 1 instead of any  $n \in \mathbb{N}$ . Thanks to inclusion neutrality, such simplifications of formal expressions induce no conservatism in the related set-valued interpretations. Other rewriting rules are only inclusion preserving:

**Proposition 30** The rewriting rules in (13), (14) and (15) are inclusion preserving under the assumption 16.

$$(|^1_0|_i) \rightarrow 1/2 + (|\pm|_j)/2, \quad (13)$$

$$(|\pm|_i) \rightarrow (\square_j), \quad (14)$$

$$(\square_i)^2 \rightarrow 1/2 + (\square_j)/2, \quad (\square_i)(\square_j) \rightarrow (\square_k). \quad (15)$$

(13)-(15) apply before computing the zonotope/interval enclosure of a (possibly mixed) polynotope. Notice that (13) is inclusion neutral if applied globally i.e. without generating new symbol multi-occurrences. (14) is the formal/syntactical counterpart of  $\{-1, +1\} \subset [-1, +1]$  which can be viewed as a prototype of the most basic inclusion of two discrete modes/configurations ( $-1$  and  $+1$ ) into a single continuous domain (the unit interval). By using appropriate reductions of formal expressions based on inclusion preserving rewriting rules, mixed polynotopes provide a highly versatile, scalable and computationally efficient framework to combine and enclose possibly non convex and non connected sets under dependency constraints. Hence, they look appealing to deal with verification and synthesis of Cyber-Physical Systems (CPS) whose modeling often relies on mixed/hybrid dynamics. They also exemplify the generality of the framework of image sets with typed symbols formalized in section 3.

## 5 Modeling tools for nonlinear hybrid systems

### 5.1 Discrete: Signed and Boolean logic functions

This paragraph shows how signed (resp. boolean) symbolic variables can be used in a polynomial framework, like the one of polynotopes under the assumption 16, to express any propositional logic formula where symbolic variables are interpreted on a bi-valued real domain:  $\boxplus = \{-1, +1\} \subset \mathbb{R}$  (resp.  $\{0, 1\} \subset \mathbb{R}$ ). This gives a natural interface between continuous variables (defined on a (real) domain with infinite cardinal) and discrete ones (defined on a (real) domain with finite cardinal).

**Proposition 31 (Multi-affine decomposition)** *Let  $f : \mathbb{R}^p \rightarrow \mathbb{R}^n$  be any function between finite dimensional real domains. Let  $x \in \mathbb{R}$  and  $z \in \mathbb{R}^{p-1}$  so that  $(x, z) \in \mathbb{R}^p$  refers to any input vector of  $f$  where a scalar input  $x$  is distinguished from the others. Let introduce four partial functions of  $f$  defined as:*

$$f_x^A(z) = \frac{f(+1, z) + f(-1, z)}{2} : \text{Average of } f \text{ wrt } x,$$

$$f_x^H(z) = \frac{f(+1, z) - f(-1, z)}{2} : \text{Half-gap of } f \text{ wrt } x,$$

$$f_x^G(z) = f(0, z) : \text{Ground of } f \text{ wrt } x,$$

$$f_x^U(z) = f(1, z) - f(0, z) : \text{Unit-gap of } f \text{ wrt } x,$$

Then, an affine decomposition of  $f$  wrt  $x$  under a signed (resp. boolean)  $x$  is respectively given by (16) and (17). Moreover, if all the scalar entries of  $z$  are signed (resp. boolean), a recursive application of (16) (resp. (17)) results in a (polynomial) multi-affine decomposition of  $f$ .

$$x \in \{-1, +1\} \Rightarrow f(x, z) = f_x^A(z) + x f_x^H(z), \quad (16)$$

$$x \in \{0, 1\} \Rightarrow f(x, z) = f_x^G(z) + x f_x^U(z). \quad (17)$$

Proof: (16) comes from  $f(+1, z) = f_x^A(z) + f_x^H(z)$  and  $f(-1, z) = f_x^A(z) - f_x^H(z)$ . Similarly, (17) comes from

Table 1

Signed and Boolean logic functions related to basic operators expressed in the ring of multivariate polynomials  $\mathbb{R}[s_I]$  with coefficients in the real field  $(\mathbb{R}, +, \cdot)$ .

| Op.   | Symb.                    | $\in \{-1, +1\}^2$    | $\in \{0, 1\}^2$      |
|-------|--------------------------|-----------------------|-----------------------|
| not   | $\neg$                   | $-a$                  | $1 - a$               |
| and   | $\wedge$                 | $\frac{-1+a+b+ab}{2}$ | $ab$                  |
| or    | $\vee$                   | $\frac{+1+a+b-ab}{2}$ | $a + b - ab$          |
| nand  | $\uparrow, \bar{\wedge}$ | $\frac{+1-a-b-ab}{2}$ | $1 - ab$              |
| nor   | $\downarrow, \bar{\vee}$ | $\frac{-1-a-b+ab}{2}$ | $1 - a - b + ab$      |
| imp   | $\Rightarrow, \leq$      | $\frac{+1-a+b+ab}{2}$ | $1 - a + ab$          |
| eqv   | $\Leftrightarrow, =$     | $ab$                  | $1 - a - b + 2ab$     |
| xor   | $\oplus, \neq$           | $-ab$                 | $a + b - 2ab$         |
| pow   | $a^n, n \in \mathbb{N}$  | $a^{\text{mod}(n,2)}$ | $a^{\text{max}(n,1)}$ |
| true  | $\top$                   | $+1$                  | $1$                   |
| false | $\perp$                  | $-1$                  | $0$                   |

$$f(0, z) = f_x^G(z) \text{ and } f(1, z) = f_x^G(z) + f_x^U(z).$$

The multi-affine decomposition of basic propositional logic operators is reported in Table 1 both in the signed and boolean cases. At least three noticeable facts emerge from Table 1:

a) The equivalence  $\text{eqv}$  in the signed case features the same multi-affine decomposition as the logical  $\text{and}$  in the boolean case, and both reduce to a simple product.

b) The multi-affine decompositions with signed operands look more “balanced” in terms of involved monomials, compared to the boolean case. This is visible right from the basic affine decompositions in (16) and (17). Indeed, the average of both alternatives (resp. the 0 alternative) serve as reference to express the impact of a switching controlled by  $x$  in the signed (resp. boolean) case.

c) Interpreting in  $\mathbb{R}$  the polynomial expression of a multi-affine decomposition yields some interpolation between discrete configurations initially expressed in a (bi-valued) propositional logic framework.

**Proposition 32 (Logical ordering)** *Let  $(a, b)$  be a pair of signed (resp. boolean) symbolic variables. Defining the operator  $>$  such that  $(a > b) = \neg(a \leq b)$  holds true with operators as in table 1, then  $(a < b) = (b > a)$  and  $(a \leq b) = ((a < b) \vee (a = b))$  also hold true. More generally, the operators  $\leq$  (i.e. implication<sup>13</sup>),  $\geq$ ,  $>$ ,  $<$  follow similar rules as classical order relation operators over reals when signed (resp. boolean) symbols are interpreted with values in  $\{-1, +1\} \subset \mathbb{R}$  (resp.  $\{0, 1\} \subset \mathbb{R}$ ).*

**Theorem 33 (Functional completeness)** *Under the assumption 16, let  $I \subset \mathbb{N}$  be a finite set of unique symbol identifiers ( $I = \mathbb{N}$ ) with at least  $p$  elements of type signed (resp. boolean).  $s$ -polynotopes based on wff interpreted*

<sup>13</sup> Notice that contraposition writes as  $(a \leq b) = (\neg b \leq \neg a)$ .

as multivariate polynomials  $\mathbb{R}[s_I]$  with coefficients in the real field  $(\mathbb{R}, +, \cdot)$  can describe any function  $f : \boxplus^p \rightarrow \boxplus$  (resp.  $f : |_0^1|^p \rightarrow |_0^1$ ), where  $\{\pm\} = \{-1, +1\} \subset \mathbb{R}$  (resp.  $|_0^1| = \{0, 1\} \subset \mathbb{R}$ ).

**PROOF.** Theorem 33 follows from the functional completeness of the nand (or nor) logical operator and the fact that the composition of polynomials in  $\mathbb{R}[s_I]$  result in polynomials in  $\mathbb{R}[s_I]$ . Indeed, the nand operator is defined as a polynomial function with signed (resp. boolean) operands and codomain in Table 1. Thus, the composition of any number of such nand operations on signed (resp. boolean) symbolic variables evaluated in  $|\pm|$  (resp.  $|_0^1|$ ) result in a polynomial s-function i.e. a s-polynotope according to the definition 26.

**Corollary 34** *Given any pair  $(a, b) \in \mathbb{R}^2$  satisfying  $a < b$ , all the finite dimensional Boolean functions and operations can be plunged in  $\{a, b\}^p \subset \mathbb{R}^p$  for some  $p \in \mathbb{N}$  after suitable re-scaling compared to the usual Boolean case i.e.  $(a, b) = (0, 1)$ . This is exemplified with the so-called signed case i.e.  $(a, b) = (-1, +1)$  in table 1, where the direct and inverse affine re-scaling functions are  $r : \boxplus \rightarrow |_0^1|, x \mapsto \frac{1+x}{2}$  and  $r^{-1} : |_0^1| \rightarrow \boxplus, x \mapsto 2x - 1$ .*

## 5.2 Continuous: Nonlinear functions

Whereas the imset (see definition 1) of a polynotope (resp. zonotope) by a polynomial (resp. affine) function is still a polynotope (resp. zonotope), the imset by non-polynomial (resp. non-linear) functions is not. This paragraph proposes a method to obtain guaranteed inclusions of non-polynomial (resp. non-linear) functions while maintaining dependency links between inputs and outputs. Indeed, breaking such links (e.g. by a naive use of interval arithmetic) is often the source of over-approximations and/or wrapping effect.

For the sake of simplified notations, the distinction between s-functions (syntax) and their usual interpretation as a mathematical function (semantic) is not systematic in the following. Example: Let  $f(x) = e^x$ . Then,  $f$  refers either to the s-function built from the wff  $e^x$ , or to  $\iota_m f : x \mapsto e^x$ .

The notations used for intervals are as follows:  $x \in [x] = [\underline{x}, \bar{x}] = \hat{x} \pm \dot{x} = [\hat{x} - \dot{x}, \hat{x} + \dot{x}]$  where  $\underline{x}, \bar{x}, \hat{x}, \dot{x}$  respectively denote the lower bound, upper bound, center (or middle), radius of the interval  $[x]$  containing  $x$ . Then,  $\hat{x} = \frac{\bar{x} + \underline{x}}{2}$  and  $\dot{x} = \frac{\bar{x} - \underline{x}}{2}$ . Recall:  $\square = [-1, +1]$ .

**Lemma 35 (Unit range mapping)** *Let  $[x] = [\underline{x}, \bar{x}] = \hat{x} \pm \dot{x} \subset \mathbb{R}$ . Let  $\mu : [x] \rightarrow \square, x \mapsto \delta = \frac{\underline{x} - \hat{x}}{\dot{x}}$  if  $\dot{x} \neq 0$ ,  $\delta = 0$  otherwise.  $\mu^{-1}(\delta) = \hat{x} + \dot{x}\delta$ . Unless  $\dot{x} = 0$  (degenerate punctual case), the unit range mapping  $\mu$  (or  $\mu_{[x]}$ ) of  $[x]$  is linear and bijective: It maps the interval range  $[x]$  of  $x$  to the unit interval  $\square$  containing any  $\delta = \mu(x), x \in [x]$ .*

Given an interval  $[x] \subset \mathbb{R}$ , let  $f : [x] \rightarrow \mathbb{R}, x \mapsto y = f(x)$  be a function that does not satisfy a property  $\pi$  (i.e.  $\neg\pi(f)$  is true) required for a given class of image-sets to be closed under the (element-wise) application of  $f$  to the underlying s-functions. For example:  $\pi$  being the property of being linear (resp. polynomial), the class of e-zonotopes (resp. e-polytopes) are closed under the application of linear (resp. polynomial) functions to the underlying s-zonotopes (resp. s-polytopes).  $\neg\pi(f)$  then means that  $f$  is non-linear (resp. non-polynomial) for zonotopes (resp. polynotopes). The considered structural property  $\pi$  is assumed to be preserved through function composition.

**Lemma 36 (Generic inclusion method)** *Given an interval  $[x] \subset \mathbb{R}$  and  $f : [x] \rightarrow \mathbb{R}, x \mapsto y = f(x)$  with  $\neg\pi(f)$ . Let  $g : \square^2 \rightarrow \mathbb{R}, (\delta, \epsilon) \mapsto g(\delta, \epsilon)$  be a function satisfying  $\forall x \in [x], \exists \epsilon \in \square, f(x) = g(\mu(x), \epsilon)$ , where  $\mu$  is the unit range mapping of  $[x]$ . Then,  $\tilde{f}(\cdot) = g(\mu(\cdot), \square)$  is an inclusion function for  $f(\cdot)$ . Also,  $\pi(g) \wedge \pi(\mu) \Rightarrow \pi(\tilde{f})$ .*

According to Lemma 36, enclosing a non-linear (resp. non-polynomial) function  $f$  in a linear (resp. polynomial) framework can be achieved by finding an adequate linear (resp. polynomial) function  $g$ . In order to exemplify the generic inclusion method, a more focused approach is proposed for increasing/decreasing and convex/concave functions  $f$  on some interval  $[x]$ . Notation:

$$[\partial_x f](\cdot) = \left. \frac{\partial f(x)}{\partial x} \right|_{x=\cdot}.$$

**Theorem 37 (An inclusion method)** *Let  $f : [x] \rightarrow \mathbb{R}, x \mapsto y = f(x)$  be a class  $\mathcal{C}^1$  convex or concave function on a given interval  $[x] = \hat{x} \pm \dot{x} = [\underline{x}, \bar{x}] \subset \mathbb{R}$  with  $\dot{x} > 0$ . Let  $y = f(\underline{x}), \bar{y} = f(\bar{x}), \hat{y} = (\bar{y} + \underline{y})/2, \dot{y} = (\bar{y} - \underline{y})/2$ . Let  $\delta = \mu(x)$  where  $\mu$  is the unit range mapping of  $[x]$  (so,  $x \in [x] \Leftrightarrow \delta \in \square$ ). Let  $r(\delta) = f(\hat{x} + \dot{x}\delta) - (\hat{y} + \dot{y}\delta)$ . Let  $\delta^*$  be the solution of  $[\partial_x f](\hat{x} + \dot{x}\delta^*) = \dot{y}/\dot{x}$ . Then,  $g(\delta, \epsilon) = g_0 + g_1\delta + g_2\epsilon$  with  $g_0 = \hat{y} + \frac{1}{2}r(\delta^*)$ ,  $g_1 = \dot{y}$ ,  $g_2 = \frac{1}{2}|r(\delta^*)|$  satisfies  $\forall x \in [x], \exists \epsilon \in \square, f(x) = g(\mu(x), \epsilon)$ .  $\tilde{f}(\cdot) = g(\mu(\cdot), \square)$  is an inclusion function for  $f(\cdot)$  on  $[x]$ .*

**PROOF.** The regularity of  $f$  on  $[x]$  ensures that  $[\partial_x r](\delta^*) = 0$  i.e.  $[\partial_x f](\hat{x} + \dot{x}\delta^*) = \dot{y}/\dot{x}$  has a unique solution. Since  $r(-1) = r(+1) = 0$ , if  $f$  is convex (resp. concave) on  $[x]$ , then  $r(\delta) \in [r(\delta^*), 0]$  (resp.  $r(\delta) \in [0, r(\delta^*)]$ ) for  $\delta \in \square$ . The two cases are gathered as:  $r(\delta) \in \frac{1}{2}r(\delta^*) \pm \frac{1}{2}|r(\delta^*)|$ . Thus,  $\exists \epsilon \in \square, r(\delta) = f(x) - (\hat{y} + \dot{y}\delta) = \frac{1}{2}r(\delta^*) + \frac{1}{2}|r(\delta^*)|\epsilon$ , as  $x = \hat{x} + \dot{x}\delta$  by definition of  $\mu$  as in Lemma 35. Then,  $g(\delta, \epsilon)$  and the proof follow from the last equality.

**Corollary 38** *The s-function  $[\mu^{-1}(\delta); g(\delta, \epsilon)]$  where  $\delta$  and  $\epsilon$  refer to symbols of type (unit) interval is a continuous s-zonotope since  $\mu^{-1}$  and  $g$  are affine.  $\forall x \in [x], [x; f(x)] \in \langle [\mu^{-1}(\delta); g(\delta, \epsilon)] \rangle_{s, \tau, \iota}$ , an e-zonotope usually not reduced to an aligned box due to the dependency*

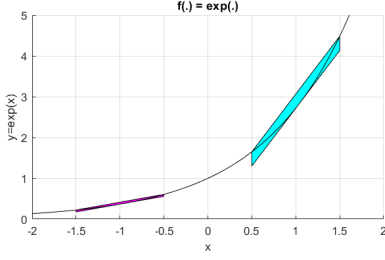


Fig. 3. Inclusion method of theorem 37 applied to  $f(x) = e^x$  on  $[x] = -1 \pm 0.5$  (magenta) and  $[x] = +1 \pm 0.5$  (cyan): plot of e-zonotopes as in corollary 38.  $\hat{x} + \dot{x}\delta^* = \log(\dot{y}/\dot{x})$ .

of both dimensions on common symbol(s) referred as  $\delta$ . Moreover, if  $x$  is a polynotope, so is  $\langle [\mu^{-1}(\delta); g(\delta, \epsilon)] \rangle_{s, \tau}$ .

An illustrative example with  $f(x) = e^x$  is reported in Fig. 3 and further remarks are reported hereafter:

- a) The inclusion proposed in theorem 37 is entirely parameterized by the input domain  $[x]$  while not being subject to the arbitrary choice of a point used as reference for linearizing or computing a Taylor expansion.
- b)  $\delta^*$  often has an explicit form, e.g.,  $\hat{x} + \dot{x}\delta^* = \log(\dot{y}/\dot{x})$ ,  $\dot{x}/\dot{y}$ ,  $\frac{1}{4}(\dot{x}/\dot{y})^2$  for  $f(x) = e^x$ ,  $\log(x)$ ,  $\sqrt{x}$ , respectively.
- c) If  $\dot{x} = 0$ , then the input is punctual and  $f(x) = f(\hat{x})$ . This is consistent with the limit  $\dot{x} \rightarrow 0$  since the continuity of  $f$  gives  $\dot{y} \rightarrow 0$ ,  $g_0 \rightarrow \dot{y}$ ,  $g_1 \rightarrow 0$  and  $g_2 \rightarrow 0$ .
- d) If  $f$  is decreasing, then  $\dot{y} < \dot{y}$  and  $\dot{y} < 0$  in theorem 37.
- e)  $r(\delta)$  is the remainder term wrt to a (linear) approximation of  $f(x)$  which itself (linearly) depends on  $x$ :  $\dot{y} + \dot{y}\mu(x)$ . The purpose of a dependency-preserving inclusion (dpi) is thus achieved, at least for a structural property  $\pi$  referring to being linear. Note that polynomial dependencies possibly modeling  $x$  (then,  $x(\cdot)$  and  $\delta(\cdot) = \mu(x(\cdot))$  are polynomials) are readily propagated by a linear enclosing approximation  $\tilde{f}(\cdot)$  of  $f(\cdot)$ . Indeed, the composition of affine and polynomial functions is still polynomial. Thus, the result in theorem 37 is readily applicable with polynotopes. Moreover, the generic inclusion method in Lemma 36 encompasses polynomial enclosing approximations of non-polynomial functions.

### 5.3 Hybrid: Switching functions

In the last paragraph (§5.2), an inclusion method for functions  $f$  satisfying the regularity conditions of being  $\mathcal{C}^1$  has been proposed in Theorem 37. Following the generic inclusion method stated in Lemma 36, the case of a prototypical  $\mathcal{C}^0$  but not  $\mathcal{C}^1$  function is considered in this paragraph: the absolute value. The motivation for this is summarized in Table 2 which shows that several useful switching functions can be built by composing basic operators (like  $+$ ,  $-$ , taking the half) with the absolute value operator  $abs(x) = |x|$ . Thus, a dependency-preserving inclusion of a prototypical switching function like  $abs$  is highly desirable to model and efficiently propagate uncertainties within hybrid dynamical systems,

Table 2  
Switching functions expressed from the absolute value operator:  $abs(x) = |x|$  (or from ReLU\*).

| Function   | Notation                         | Expression with $ . $ (or pos)                                     |
|------------|----------------------------------|--|
| Maximum    | $\max(x, y)$                     | $= \frac{x+y}{2} + \frac{ x-y }{2} (= y + pos(x-y))$               |
| Minimum    | $\min(x, y)$                     | $= \frac{x+y}{2} - \frac{ x-y }{2} (= x - pos(x-y))$               |
| Saturation | $sat(x, \underline{x}, \bar{x})$ | $= \frac{1}{2}(x + \bar{x} +  \underline{x} - x  -  x - \bar{x} )$ |
| Deadzone   | $dz(x, \underline{x}, \bar{x})$  | $= x - sat(x, \underline{x}, \bar{x})$                             |
| ReLU*      | $pos(x)$                         | $= \max(0, x) = \frac{x+ x }{2}$                                   |

\*Rectifier Linear Unit (remark:  $|x| = 2pos(x) - x$ ).

without necessarily requiring costly bisections and/or a specific management of guard conditions.

**Theorem 39 (An inclusion of abs)** *Let  $abs : [x] \rightarrow \mathbb{R}$ ,  $x \mapsto y = |x|$  be the restriction of the absolute value on a given interval  $[x] = \hat{x} \pm \dot{x} = [\underline{x}, \bar{x}] \subset \mathbb{R}$ .*

*Case 1: If  $\bar{x} \leq 0$ , then  $abs(\cdot) = -(\cdot)$ ,*

*Case 2: If  $\underline{x} \geq 0$ , then  $abs(\cdot) = +(\cdot)$ ,*

*Case 3: If  $|\hat{x}| < \dot{x}$ , then  $abs(\cdot)$  is an inclusion function for  $abs(\cdot)$  on  $[x]$  with:*

$$\widetilde{abs}(\cdot) = \left( \frac{\hat{x}}{\dot{x}} \right) (\cdot) + \left( \frac{\dot{x}^2 - \hat{x}^2}{2\dot{x}} \right) (1 + \square). \quad (18)$$

**PROOF.** If  $0 \notin [x]$  (case 1 or 2),  $abs(\cdot)$  is linear and no dedicated inclusion is then required. If  $0 \in [x]$  (case 3), the inclusion method of theorem 37 is applied step-by-step: Let  $\mu$  be the unit range mapping of  $[x]$  and  $\delta = \mu(x)$ . Since  $abs(\cdot)$  is only  $\mathcal{C}^0$  and convex on  $[x]$ , but not  $\mathcal{C}^1$ , the range of the remainder  $r(\delta) \leq 0$  (still such that  $r(-1) = r(+1) = 0$ ) is computed by noticing that its minimum is obtained for  $x = \hat{x} + \dot{x}\delta^* = 0$ . Then,  $\delta^* = -\hat{x}/\dot{x}$  gives  $r(\delta^*) = (\hat{x}^2 - \dot{x}^2)/\dot{x}$  and satisfies  $\forall \delta \in \square, r(\delta) \in [r(\delta^*), 0]$ . It comes  $g(\delta, \epsilon) = g_0 + g_1\delta + g_2\epsilon$  with  $g_0 = \frac{\dot{x}^2 + \hat{x}^2}{2\dot{x}}$ ,  $g_1 = \hat{x}$ ,  $g_2 = \frac{\dot{x}^2 - \hat{x}^2}{2\dot{x}}$  ( $|\hat{x}| < \dot{x}$  in case 3). Finally,  $g(\mu(x), \epsilon) = (\frac{\hat{x}}{\dot{x}})x + (\frac{\dot{x}^2 - \hat{x}^2}{2\dot{x}})(1 + \epsilon)$ .

Corollary 38 still applies to  $f = abs$ , as a corollary of theorem 39 rather than theorem 37. A dependency-preserving inclusion of  $abs(\cdot)$  has been obtained. By extension, dependency-preserving inclusions (dpi) for the switching functions reported in table 2, among others possibly resulting from functional compositions are also obtained. Moreover, the vertical concatenation operator implemented for zonotopes and polynotopes allows to build  $n$ -dimensional dpi from scalar ones through basic compositions. These can be implemented by using the overloading capability of some object oriented languages, to the benefit of code readability. This feature holds not only for switching functions, but also for non-linear/non-polynomial ones. This makes polynotopes a relevant tool to compute and analyze mixed uncertainty propagation within non-linear hybrid dynamical systems.

cal systems. Indeed, their polynomial nature, efficiently encoded by combining full and sparse data structures, looks appropriate to model a wide spectrum of non-trivial dependencies, as shown by the functional completeness result given in theorem 33.

## 6 Polynotopic Kalman Filter (PKF)

An extension of Kalman Filtering to discrete-time non-linear hybrid dynamical systems is proposed in this section. It is based on polynotopes and interpretations related to a set-membership uncertainty paradigm.

Let  $x(s)$  be a s-polynotope (7):  $x(s) = \langle c, R, I, E \rangle_{s,\tau} = c + R s_I^E$  (syntax). By analogy with zonotopes, its covariation [13] is defined as:  $\text{cov}(x(s)) = RR^T$ . In order to possibly take symbol types and/or the monomial structure into account, a covariation weighted by  $\Phi$  (or  $\Phi(\cdot)$ ) is introduced as:

**Definition 40 (Weighted covariation)** *Given a symmetric matrix  $\Phi$  ( $\Phi = \Phi^T$ ), the weighted covariation of  $\mathbf{x} = \langle c, R, \dots \rangle_{s,\tau(\cdot)}$  (polynotope or zonotope) is:*

$$\text{cov}_\Phi(\mathbf{x}) = R\Phi R^T.$$

$x(s)$  formalizes a polynomial (s-)function of the symbolic variables in  $s_I$ . The execution of polynotope operations like sum, linear image, concatenation, reduction, zonotopic hull  $\mathcal{Z}x(s)$ , interval/box hull  $\mathcal{B}x(s)$ , etc mainly work at a syntactic level by manipulating polynomial expressions (e.g. encoded as  $(c, R, I, E)$  with sparse  $E$ ) while preserving semantic properties. In particular, inclusion is viewed as a semantic property related to a set-membership interpretation of polynomial functions depending on typed<sup>14</sup> symbolic variables. From (8), it comes:  $\forall \sigma \in \iota\tau s_I, \iota x(\sigma) \in \mathcal{P}x(s) = \langle c, R, I, E \rangle_{s,\tau,\iota}$  (semantics), where  $\iota x(\cdot)$  stands for the interpretation of  $x(\cdot)$  as a vector of polynomial mathematical functions  $(\mathbb{R}^{\dim(I)} \rightarrow \mathbb{R})$  with real coefficients (under assumption 16). Since probability theory is the most commonly used framework for nonlinear filtering, some analogies and possible links are briefly outlined:

**Conjecture 41 (probability measure)**  $\sigma$  (as in definition 9, (4) and (8)) can be viewed as an “outcome”, the function  $\iota x(\cdot)$  as a “random variable”,  $[\iota x]^{-1}(S)$  as an “event” related to any set  $S$  of output values taken by  $\iota x(\cdot)$ . A “measure”  $\pi(\cdot)$  of events on the domain  $\iota\tau s_I$  induced by an interpretation of symbol types becomes a “probability measure” as long as  $\pi(\iota\tau s_I) = 1$ . The typed symbols  $s_I$  then contribute to define the probability space.

**Remark 42** Another way to introduce probability theory in the proposed framework consists in extending the

<sup>14</sup> Notice that the set-membership interpretation is also related to the types considered under the assumption 16.

symbol types considered in assumption 16 to other types like (some class of) random variables defined on a given probability space (e.g. see §2.2 and definition 6.1 in [17]).

In the following, no probability measure is considered. Notations:  $\mathbf{x} = x(s)$  denotes a s-polynotope.  $x = \iota x(\sigma) \in \mathbb{R}^n$  denotes a punctual evaluation of  $\mathbf{x}$  obtained for some so-called outcome  $\sigma \in \iota\tau s_I$ . Then,  $x \in \mathcal{P}\mathbf{x}$ , the e-polynotope related to  $\mathbf{x}$ . Also,  $x \in \mathcal{Z}\mathbf{x}$  (resp.  $x \in \mathcal{B}\mathbf{x}$ ) means that  $x$  belongs to a zonotopic (resp. interval/box) hull of  $\mathbf{x}$ .

The state observation (or filtering) problem addressed in this section deals with discrete-time non-linear hybrid dynamical systems modeled as:

$$x_+ = f(x, u, v), \quad x_0 \in \mathcal{P}\mathbf{x}_0, v \in \mathcal{P}\mathbf{v}, \quad (19)$$

$$0 = g(x, u, v, y), \quad (20)$$

where the functions  $f(\cdot)$  and  $g(\cdot)$  result from the composition of elementary functions and operators for which inclusion preserving polynotope versions are available. In practice, this is not much restrictive since sum, linear image, reduction, concatenation, product are available (see §4.3) and the modeling tools for nonlinear hybrid systems developed in section 5 can be used to that purpose. Then, by overloading<sup>15</sup> these elementary functions and operators with their inclusion preserving polynotopic version, and by applying the same composition, inclusion functions with polynotopic inputs and outputs  $\tilde{f}(\cdot)$  and  $\tilde{g}(\cdot)$  can be obtained for  $f(\cdot)$  and  $g(\cdot)$ , respectively. In (19), the index + refers to the next time step  $k+1$  and the current time step  $k$  is omitted to simplify the notations, except for the initial state  $x_0$  at time  $k=0$ .  $x_0 \in \mathbb{R}^{n_x}$  is assumed unknown but bounded by the e-polynotope  $\mathcal{P}\mathbf{x}_0$  related to a known s-polynotope  $\mathbf{x}_0$ .  $x \in \mathbb{R}^{n_x}$ ,  $u \in \mathbb{R}^{n_u}$ ,  $y \in \mathbb{R}^{n_y}$ ,  $v \in \mathbb{R}^{n_v}$  respectively stand for the states, the known (control) inputs, the known measurements, the unknown but bounded uncertainties (state and measurement noises, disturbances, modeling errors, etc) at time  $k$ .  $v$  is assumed bounded by a known polynotope  $\mathcal{P}\mathbf{v}$ . Notice that  $u \in \mathcal{P}\mathbf{u} = \{u\}$  (singleton) for  $\mathbf{u} = \langle u, \emptyset, \emptyset, \emptyset \rangle_{s,\tau}$ . Similarly,  $y \in \mathcal{P}\mathbf{y}$  with  $\mathbf{y} = \langle y, \emptyset, \emptyset, \emptyset \rangle_{s,\tau}$ . The problem addressed is that of designing a one step-ahead prediction filter (or state observer) minimizing the trace  $\text{tr}(\cdot)$  of the (weighted) covariation of a polynotope enclosing the predicted state.

Filtering is mainly a data fusion process. So, how to merge (vector) sources ? Weighting is a usual solution:

$$z_1 \in \mathcal{P}\mathbf{z}_1 \wedge z_2 \in \mathcal{P}\mathbf{z}_2 \Rightarrow z = G_1 z_1 + G_2 z_2 \in \mathcal{P}\mathbf{z}$$

$$\text{with } \mathbf{z} = G_1 \mathbf{z}_1 + G_2 \mathbf{z}_2. \quad (21)$$

Two noticeable ways to particularize (21) are:

a) Taking  $z_1 = z_2$  under  $G_1 + G_2 = \mathcal{I}$  gives (22) which

<sup>15</sup> To the benefit of code readability and maintainability.

Table 3  
PKF iteration:  $\mathbf{x}_+ = \text{PKF}(\mathbf{x}, \mathbf{u}, \mathbf{v}, \mathbf{y}, \tilde{f}, \tilde{g}, \Phi, q)$ :

$$\begin{aligned}
\bar{\mathbf{x}} &= \downarrow_q \mathbf{x}, & \text{reduction} & (24) \\
\mathbf{p} &= \tilde{f}(\bar{\mathbf{x}}, \mathbf{u}, \mathbf{v}), & \text{prediction} & (25) \\
\mathbf{e} &= \tilde{g}(\bar{\mathbf{x}}, \mathbf{u}, \mathbf{v}, \mathbf{y}), & \text{innovation} & (26) \\
\left\langle \check{c}, \begin{bmatrix} R_p \\ R_e \end{bmatrix}, \check{I}, \check{E} \right\rangle_{s,\tau} &= \begin{bmatrix} \mathbf{p} \\ \mathbf{e} \end{bmatrix}, & \text{alignment} & (27) \\
G &= (R_p \Phi R_e^T)(R_e \Phi R_e^T)^{-1}, & \text{optimal gain} & (28) \\
\mathbf{x}_+ &= \mathbf{p} - G\mathbf{e}. & \text{update} & (29)
\end{aligned}$$

parameterizes enclosures of a polynotope intersection that could be used to design a state bounding observer:

$$z \in (\mathcal{P}\mathbf{z}_1 \cap \mathcal{P}\mathbf{z}_2) \Rightarrow z \in \mathcal{P}(G_1\mathbf{z}_1 + G_2\mathbf{z}_2). \quad (22)$$

$$z \in \mathcal{P}\mathbf{z}_1 \wedge 0 \in \mathcal{P}\mathbf{z}_2 \Rightarrow z \in \mathcal{P}(\mathbf{z}_1 - G\mathbf{z}_2). \quad (23)$$

b) Taking  $z_2 = 0$  and  $G_1 = \mathcal{I}$  under  $G_2 = -G$  gives (23) which parameterizes an update (or correction) of an initial knowledge  $\mathcal{P}\mathbf{z}_1$  about  $z$  with some other depending knowledge,  $\mathcal{P}\mathbf{z}_2$ , such as the one obtained through some measurements. (23) thus looks as a prototypical weighting underlying the structure of Kalman Filters. Moreover, in our framework, the symbols possibly shared between  $\mathbf{z}_1$  and  $\mathbf{z}_2$  play a key role in the modeling of dependencies. This makes it possible to tune/optimize  $G$  so as to maximize uncertainty cancellation<sup>16</sup> when computing  $\mathbf{z}_1 - G\mathbf{z}_2$ . The general idea of Kalman Filters is indeed to optimize the precision of a prediction  $\mathbf{p} = \mathbf{z}_1$  by using a dependent yet complementary source, the innovation  $\mathbf{e} = \mathbf{z}_2$ , to update the prediction as  $\mathbf{p} - G\mathbf{e}$  (29). Then, the algorithm (24)-(29) implementing an iteration of the proposed Polynotopic Kalman Filter (PKF) follows as in Table 3 and theorem 43.

#### Theorem 43 (PKF: inclusion and optimal gain)

Given a system modeled as in (19)-(20), the PKF iteration in (24)-(29) (Table 3) satisfies a) and b):

- a)  $x \in \mathcal{P}\mathbf{x} \wedge v \in \mathcal{P}\mathbf{v} \Rightarrow x_+ \in \mathcal{P}\mathbf{x}_+$ ,
- b) Let  $G^* = \arg \min_G \text{tr}(\text{cov}_\Phi(\mathbf{x}_+))$ .  $G^*$  is the optimal gain computed as in (28):  $G^* = (R_p \Phi R_e^T)(R_e \Phi R_e^T)^{-1}$ .

**PROOF.** a) : By construction,  $\tilde{f}(\cdot)$  and  $\tilde{g}(\cdot)$  are inclusion functions for  $f(\cdot)$  and  $g(\cdot)$ . Since the reduction step (24) is inclusion preserving, the inclusion property a) is a direct consequence of (23) with  $\mathbf{z}_1 = \mathbf{p}$  and  $\mathbf{z}_2 = \mathbf{e}$ .  
b) :  $\partial_X h(X)$  denoting  $\partial h(X)/\partial X$ , if  $h(\cdot)$  returns scalar values and  $X = [X_{ij}]$  is a matrix, then  $\partial_X h(X) =$

<sup>16</sup> which is impossible with usual interval arithmetic, subject to the so-called dependency problem.

$[\partial_{X_{ji}} h(X)]$ .  $X, A, B, C$  being matrices of correct size,

$$\partial_X \text{tr}(AX^T B) = A^T B^T, \quad (30)$$

$$\partial_X \text{tr}(AXBX^T C) = BX^T CA + B^T X^T A^T C^T. \quad (31)$$

Let  $J(G) = \text{tr}(\text{cov}_\Phi(\mathbf{x}_+))$ . In (27),  $\check{c} = [c_p; c_e]$  and  $[\mathbf{p}; \mathbf{e}]$  is such that<sup>17</sup>  $\mathbf{p} = c_p + R_p s_{\check{I}}^{\check{E}}$  and  $\mathbf{e} = c_e + R_e s_{\check{I}}^{\check{E}}$ . From (29),  $\mathbf{x}_+ = \langle c_p - Gc_e, R_p - GR_e, \check{I}, \check{E} \rangle_{s,\tau}$  and  $J(G) = \text{tr}((R_p - GR_e)\Phi(R_p - GR_e)^T) = \text{tr}(R_p \Phi R_p^T) - 2\text{tr}(R_p \Phi R_e^T G^T) + \text{tr}(GR_e \Phi R_e^T G^T)$ . Using (30) and (31),  $\partial_G J(G) = -2(R_e \Phi R_p^T) + 2(R_e \Phi R_e^T)G^T$ .  $G^*$  being the value of  $G$  such that  $\partial_G J(G) = 0$ , it comes  $G^* R_e \Phi R_e^T = R_p \Phi R_e^T$  and  $G^* = (R_p \Phi R_e^T)(R_e \Phi R_e^T)^{-1}$ .

**Theorem 44 (PKF vs. ZKF)** Let consider the particular case of linear functions  $f(\cdot)$  and  $g(\cdot)$  defined as:

$$f(x, u, v) = Ax + Bu + Ev_p,$$

$$g(x, u, v, y) = Cx + Du + Fv_e - y,$$

where  $v = [v_p; v_e]$  (state noise and measurement noise), and  $A, B, C, D, E, F$  are (possibly time-varying) matrices with appropriate dimensions. Only symbols of type (unit) interval are considered and  $\Phi = \mathcal{I}$ . Also, let  $\tilde{f}(\cdot) = f(\cdot)$ ,  $\tilde{g}(\cdot) = g(\cdot)$ ,  $x_0 \in \mathcal{P}\mathbf{x}_0$  with  $\mathbf{x}_0 = \langle c_0, R_0, I_0, \mathcal{I} \rangle_{s,\tau}$  (then,  $\mathcal{P}\mathbf{x}_0 = \mathcal{Z}\mathbf{x}_0$  is a zonotope),  $v \in \mathcal{P}\mathbf{v}$  with  $\mathbf{v} = \langle 0, \mathcal{I}, I_v, \mathcal{I} \rangle_{s,\tau}$  (then,  $\mathcal{P}\mathbf{v} = \mathcal{Z}\mathbf{v} = \mathcal{B}\mathbf{v}$  is a unit hypercube). It is also assumed that  $I_0$  and all  $I_v$ 's have no common scalar elements/identifiers which are all unique (then, no symbol being shared between  $\mathbf{x}_0$  and all the  $\mathbf{v}$ 's, this is in fact an independence assumption). Then, PKF computes the same centers  $c$  (punctual state estimates) and generator/shape matrices  $R$  as ZKF in [13] would do, up to column permutations; all the computed polynotopes are also zonotopes, and the optimal gain  $G = AK$  corresponds to the usual Kalman gain  $K = \bar{P}C^T(C\bar{P}C^T + FF^T)^{-1}$  with  $\bar{P} = \bar{R}\bar{R}^T$ .

**PROOF.** Polynotopes (and zonotopes) being closed under linear transforms, taking  $\tilde{f}(\cdot) = f(\cdot)$  and  $\tilde{g}(\cdot) = g(\cdot)$  suffices to preserve inclusion when (19)-(20) is a discrete-time LTV (or LTI) model. Moreover, all the polynotope exponent matrices equaling  $\mathcal{I}$ , (s-)polynotope operations naturally reduce to (s-)zonotope operations, and the generator matrix computed by the considered reduction operator does not depend on the symbolic description. The focus of the proof is first placed on the observer structure and, then, on the optimal gain. Observer structure:

$$(24): \bar{\mathbf{x}} = \langle \bar{c}, \bar{R}, \bar{I}, \mathcal{I} \rangle_{s,\tau} = \downarrow_q \mathbf{x} \text{ where } \bar{c} = c,$$

$$(25): \mathbf{p} = A\bar{\mathbf{x}} + Bu + Ev_p, \quad \text{with } \mathbf{v}_p = [\mathcal{I}, 0]\mathbf{v},$$

<sup>17</sup> The polynotope concatenation  $[\mathbf{p}; \mathbf{e}]$  gives expressions of  $\mathbf{p}$  and  $\mathbf{e}$  such that the generators related to their common monomials (i.e. dependencies) become “aligned” in the same columns of the matrices  $R_p$  and  $R_e$ . This is the reason why (27) is called the alignment step.

(26):  $\mathbf{e} = C\bar{\mathbf{x}} + D\mathbf{u} + F\mathbf{v}_e - \mathbf{y}$ , with  $\mathbf{v}_e = [0, \mathcal{I}]\mathbf{v}$ ,  
(29):  $\mathbf{x}_+ = \mathbf{p} - G\mathbf{e}$  gives:  
 $\mathbf{x}_+ = (A\bar{\mathbf{x}} + B\mathbf{u} + E\mathbf{v}_p) + G(\mathbf{y} - (C\bar{\mathbf{x}} + D\mathbf{u} + F\mathbf{v}_e))$ , which corresponds to ((14)) i.e. the equation (14) in [13] where  $(v, w)$  stands for  $(v_p, v_e)$ . Also, just for insight:  $\mathbf{x}_+ = (A - GC)\bar{\mathbf{x}} + (B - GD)\mathbf{u} + [E, -GF]\mathbf{v} + Gy$ . Keeping in mind that the sum of two generators with the same monomial term (here: with the same symbol) is a classical vector sum, and an horizontal concatenation otherwise (see MLC in §4.1), the centers  $c_*$  and generator matrices  $R_*$  of the s-polynotopes (also s-zonotopes since  $E_* = \mathcal{I}$ ) computed in (25), (26) and (29) are<sup>18</sup>:  
(25):  $c_p = A\bar{c} + Bu$ ,  
(25):  $R_p = [A\bar{R}, E]$  since  $\bar{I} \cap I_{v_p} = \emptyset$ ,  
(26):  $c_e = C\bar{c} + Du - y$ ,  
(26):  $R_e = [C\bar{R}, F]$  since  $\bar{I} \cap I_{v_e} = \emptyset$ ,  
(29):  $c_+ = c_p - Gc_e = (A - GC)\bar{c} + (B - GD)u + Gy$ ,  
(29):  $R_+ = R_p - GR_e = [(A - GC)\bar{R}, E, -GF]$ , since  $I_{v_p} \cap I_{v_e} = \emptyset$ , but note that PKF can take dependent state and measurement noises into account with  $\mathbf{v}$ . Finally, it can be checked that  $c_+$  and  $R_+$  exactly coincide with ((15)) and ((16)), respectively, so proving that PKF reduces to the same observer structure as ZKF under the specific assumptions of theorem 44.

Optimal gain: Let  $\bar{P} = \bar{R}\bar{R}^T$  ( $= \text{cov}_{\Phi}(\bar{\mathbf{x}})$ ,  $\Phi = \mathcal{I}$ ). Respectively substituting  $[A\bar{R}, E, 0]$  and  $[C\bar{R}, 0, F]$  for  $R_p$  and  $R_e$  in (28) gives  $G = AK$  with  $K = \bar{P}C^T(C\bar{P}C^T + FF^T)^{-1}$ . Then, it can be checked that the optimal observer gain is the same as in ((21)) – ((22)).

**Remark 45 (PKF vs. KF)** *Theorem 44 (PKF vs. ZKF) can be combined with Theorem 7 (ZKF vs. KF) in [13] to make a further bridge between set-membership and stochastic paradigms. In particular, this gives the conditions under which PKF covariations and KF covariances coincide, as well as the punctual state estimates.*

Based on modeling tools for nonlinear hybrid systems developed in the proposed framework, a compositional implementation of advanced reachability and filtering algorithms preserving inclusion is made possible by using operator overloading. This is exemplified with the Polynotopic Kalman Filter (PKF) proposed in this section.

## 7 Numerical Examples

### 7.1 Discrete: Adder

The first example illustrates some connection with basic digital circuit design. The s-polynotopes (i.e. polynomial s-functions) resulting from the multi-affine decomposition of  $n$  bits binary adders only made of *nand* gates are compared depending on the type of symbol(ic variable)s used: signed or boolean as explained in §5.1.

<sup>18</sup> Up to column permutations with no impact on the interpretation.

Table 4  
Algorithm of functions building Half (H), Full 1 bit (F), and Full  $n$  bits (N) adder with *nand* gates ( $\neg x \leftrightarrow x \bar{\wedge} x$ ).

|  |                                |
|--|--------------------------------|
| $H : (a, b) \mapsto (s, c) :$  | Half-adder with 5 nand gates   |
| $t_1 \leftarrow a \bar{\wedge} b, t_2 \leftarrow a \bar{\wedge} t_1, t_3 \leftarrow t_1 \bar{\wedge} b, s \leftarrow t_2 \bar{\wedge} t_3, c \leftarrow t_1 \bar{\wedge} t_1.$ |                                |
| $F : (a, b, c_{in}) \mapsto (s, c_{out}) :$  | Full 1 bit adder with carry    |
| $(r, c_1) \leftarrow H(a, b), (s, c_2) \leftarrow H(r, c_{in}), c_{out} \leftarrow \neg c_1 \bar{\wedge} \neg c_2.$  |                                |
| $N : (A, B, c) \mapsto (S, c) :$   | Full $n$ bits adder with carry |
| for $i \leftarrow 1 \dots n(A), (S(i), c) \leftarrow F(A(i), B(i), c).$  |                                |

Table 5

Number of distinct generators/monomials of s-polynotopes representing the multi-affine decomposition of an  $n$ -bits adder (as in table 4) with either signed or boolean symbol(ic variable)s. The computation time is given in seconds (s).

| $n$     | 1   | 2    | 3    | 4    | 5    | 6    | 7    | 8   |
|---------|-----|------|------|------|------|------|------|-----|
| Signed  | 5   | 11   | 23   | 47   | 95   | 191  | 383  | 767 |
|         | (s) | 0.01 | 0.02 | 0.03 | 0.06 | 0.15 | 0.36 | 1.9 |
|         |     |      |      |      |      |      |      | 8.3 |
| Boolean | 8   | 23   | 65   | 188  | 554  | 1649 | -    | -   |
|         | (s) | 0.01 | 0.01 | 0.03 | 0.2  | 2.3  | 29   | -   |
|         |     |      |      |      |      |      |      | -   |

The binary adders architecture is described in Table 4 where  $S(i)$  refers to the projection of the s-polynotope  $S$  along the  $i$ th dimension,  $i = 1, \dots, n(S)$ . For an  $n$  bits adder,  $A = s_{1:n}$  and  $B = s_{(n+1):2n}$  each refer to a vector of  $n$  (either signed or boolean) symbolic variables representing the (unknown) bits encoding two integer operands. The e-zonotope (or e-polynotope) related to  $A$  is the set of the  $2^n$  possible input values i.e.  $\{-1, +1\}^n$  (resp.  $\{0, 1\}^n$ ) in the signed (resp. boolean) case. Idem for  $B$ . These sets are never computed explicitly: they only describe the set-valued interpretation of semi-symbolic calculi based on the  $(c, R, I, E)$  data structure used to represent s-polynotope objects. Then, building the architecture of an  $n$  bits adder by computing  $(S, c) = N(A, B)$  as in table 4 with s-polynotope overloaded operators results in the s-polynotopes  $S$  (sum result) and  $c$  (output carry) of dimension  $n$  and 1, respectively.  $S(i)$  is a polynomial with scalar coefficients giving the expression of the  $i$ th bit of  $S$  as a function of the input bits/symbols in  $A$ ,  $B$  and an input carry. A full  $n$ -bits adder has  $2n + 1$  (binary) inputs and  $n + 1$  (binary) outputs. The s-polynotope  $\tilde{S} = [S; c]$  gathering the sum result and the output carry is thus given by  $\tilde{S} = \langle \tilde{c}, \tilde{R}, \tilde{I}, \tilde{E} \rangle_{s, \tau}$  with  $\tilde{c} \in \mathbb{R}^{n+1}$ ,  $\tilde{R} \in \mathbb{R}^{(n+1) \times m(n)}$ ,  $\tilde{I} \in \mathbb{N}^{2n+1}$ ,  $\tilde{E} \in \mathbb{N}^{(2n+1) \times m(n)}$ . The number of (distinct) generators/monomials in  $\tilde{S}$ , including the center/constant term, is  $1 + m(n)$ . This number is reported in Table 5 depending on the number  $n$  of bits of the adder and the symbol types: either signed or boolean. An unexpected yet interesting result is obtained: The number of distinct monomials required to describe the full architecture of an  $n$ -bits adder is much smaller and more scalable using signed rather than boolean symbols.

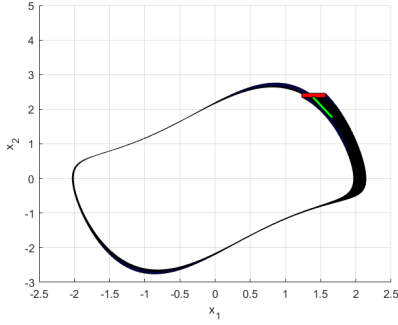


Fig. 4. Reachability result obtained on the Van-Der-Pol oscillator with continuous polynotopes (the plot results from zonotopic enclosures  $\mathcal{Z}\mathbf{x}$  at each time step).

This example of a full  $n$ -bits adder shows the ability of s-polynotopes to describe and manipulate purely discrete expressions yielding non trivial relations and dependencies between inputs and outputs. Moreover, the polynomial representation benefits from useful simplifications made possible by dealing with typed symbols.

## 7.2 Continuous: Van-Der-Pol oscillator

In order to illustrate reachability on continuous domains and compare the results with [32], a Van-Der-Pol oscillator taken from [28] is considered:

$$\begin{aligned}\dot{x}_1 &= x_2, \\ \dot{x}_2 &= (1 - x_1^2)x_2 - x_1.\end{aligned}$$

The initial state set is  $\mathcal{P}\mathbf{x}_0 = \mathcal{P}[\mathbf{x}_{1,0}; \mathbf{x}_{2,0}] = [[1.23, 1.57]; [2.34, 2.46]]$  as shown by the red box in Fig. 4. 1360 iterations based on an Euler sampling with step size  $h = 0.005$  are computed in 9.8s with continuous polynotopes under Matlab running on a 1.8 GHz Core i5 processor with 8 Go RAM. The zonotopic enclosure  $\mathcal{Z}\mathbf{x}_{1360}$  of the final polynotope (at  $t = 6.8s$ ) is the green set in Fig. 4. At each iteration, the (polynotopic version of the) reduction operator  $\downarrow_q$  from [17] with  $q = 50$  is used to: a) reduce the square  $\mathbf{x}_1^2$ , b) reduce the product  $(\mathbf{x}_1^2)\mathbf{x}_2$ , c) reduce  $\mathbf{x}$ . As expected, the reachability result shown in Fig. 4 is close to the one obtained with sparse polynomial zonotopes (spz) in the Figure 3 of [32], where a comparison with other methods is conducted. Thus, continuous polynotopes also outperform zonotopes and quadratic zonotopes on this example, which illustrates the interest in dealing with polynomial dependencies to propagate continuous domains within nonlinear dynamics.

## 7.3 Hybrid: Traffic network

In order to illustrate reachability for dynamics defined with switching functions like  $\min$  (see §5.3 and table 2) and compare the results with those reported for the

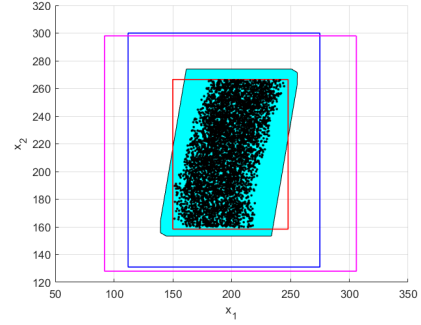


Fig. 5. Reachability result obtained with polynotopes (cyan) for the model of a 3-link traffic network representing a *diverge* junction. Comparison with the results reported in Figure 2 in [45]: methods C/GB (blue), SDMM-IA (magenta), MM and SDMM-S/F (red); Monte-Carlo simulations (black dots).

TIRA toolbox in [45], the model of a 3-link traffic network representing a *diverge* junction is considered:

$$\begin{aligned}\dot{x}_1 &= -k(x)/T + p, \\ \dot{x}_2 &= k(x)/2 - \min(c, vx_2), \\ \dot{x}_3 &= k(x)/2 - \min(c, vx_3), \\ \text{where } k(x) &= \min(c, vx_1, 2w(\bar{x} - x_2), 2w(\bar{x} - x_3)).\end{aligned}$$

$\min(., ., ., .)$  is implemented as  $\min(\min(., .), \min(., .))$ . The state  $\mathbf{x} \in \mathbb{R}^3$  is the vehicle density on each link.  $p \in [4/3, 2]$  is the constant but uncertain vehicle inflow to link 1. Notice that the constant nature of this uncertainty is naturally handled by the proposed symbolic approach (no new symbol at each time for  $\mathbf{p}$ ). As in [45], the known parameters of the network are  $[T, c, v, \bar{x}, w] = [30, 40, 0.5, 320, 1/6]$ . The initial state set is  $\mathcal{P}\mathbf{x}_0 = [[150, 200]; [180, 300]; [100, 220]]$ . An Euler sampling with step size  $h = 1$  and final time  $t_f = 30$  is considered. The reduction  $\mathbf{x} = \downarrow_q \mathbf{x}$  is applied at each iteration with  $q = 20$ . No additional information about Jacobian signs/bounds was required to compute in 0.26s the polynotope  $\mathcal{P}\mathbf{x}_{t_f}$  reported in cyan in Fig. 5. For the sake of comparison, the results in the Figure 2 in [45] are also reported in Fig. 5 : C/GB (Contraction/Growth Bound), MM (Mixed Monotonicity), SDMM-IA (Sampled Data MM-Interval arithmetic), SDMM-S/F (Sampled Data MM-Sampling/Falsification).  $\mathcal{P}\mathbf{x}_{t_f}$  looks competitive wrt to the best results obtained with TIRA (red box in Fig.5). Moreover, the computed polynotope captures the orientation of the “black cloud of sample successors” obtained from 5000 Monte-Carlo simulations and also reported in Fig. 5. This illustrates the ability of the proposed scheme to maintain dependency links while propagating uncertainties through hybrid dynamics modeled with switching functions.

## 7.4 Reachability and Filtering: Lotka-Volterra

A non-linear non-autonomous prey-predator model resulting from the discretization of a modified continuous-time Lotka-Volterra model illustrates *a*) the computation of reachable sets based on a mixed-encoding (§4.2) of the initial state set, and *b*) Polynotopic Kalman Filtering (PKF) as developed in section §6. The modified continuous-time Lotka-Volterra model is  $\dot{x} = f(x, u)$  with  $x \in \mathbb{R}^2$ ,  $u \in \mathbb{R}$ ,  $(a, b, c, d) = (2, 0.4, 1, 0.1)$ , and  $f(x, u) = [ax_1 - bx_1x_2; -cx_2 + dx_1x_2 + u]$ .

### 7.4.1 Reachability with a mixed-encoding of state sets

A mixed-encoding of the initial state set is first considered and further propagated using mixed polynotope computations within the non-linear dynamics of the discretized Lotka-Volterra model.

More precisely, following the definition 21 and the corollary 22, a 3-level signed-interval mixed encoding of the interval  $15 \pm 1$  is taken as polynotopic initial state set for both  $x_{1,0}$  and  $x_{2,0}$  (i.e.  $x_1$  and  $x_2$  at  $t = kh = 0$ ):

$$\mathbf{x}_{1,0} = 15 + 1.Z_s^3([!(3, \mathbf{s}); !(1, \mathbf{i})]), \quad (32)$$

$$\mathbf{x}_{2,0} = 15 + 1.Z_s^3([!(3, \mathbf{s}); !(1, \mathbf{i})]), \quad (33)$$

$$\mathcal{P}\mathbf{x}_0 = \mathcal{P}[\mathbf{x}_{1,0}; \mathbf{x}_{2,0}] = [[14, 16]; [14, 16]]. \quad (34)$$

Each occurrence of  $!(3, \mathbf{s})$  (resp.  $!(1, \mathbf{i})$ ) calls USP (see §3.1) which returns 3 (resp. 1) unique identifiers of symbols of type signed (resp. unit interval). Thus,  $\mathbf{x}_{1,0}$  and  $\mathbf{x}_{2,0}$  are independent since they share no common symbol. Note that the symbol types are compatible with the definition 21 of  $Z_s^g$ .  $g = 3$  means that 3 signed symbols are used to hierarchically decompose the range  $15 \pm 1$  into  $2^3 = 8$  sub-intervals. The coverage of the continuous domain  $15 \pm 1$  is then ensured by the remainder term modeled by the symbol of type unit interval uniquely identified by  $!(1, \mathbf{i})$ . For instance, let  $I = [!(3, \mathbf{s}); !(1, \mathbf{i})]$  and  $\mathbf{x}_{1,0} = 15 + 1.Z_s^3(I)$  as in (32). Then,  $\mathbf{x}_{1,0} = \langle 15, [\frac{1}{2}, \frac{1}{4}, \frac{1}{8}, \frac{1}{8}], I, 1 \rangle_{s, \tau} = \frac{1}{2}s_{I_1} + \frac{1}{4}s_{I_2} + \frac{1}{8}s_{I_3} + \frac{1}{8}s_{I_4}$ , where the 3 symbols  $s_{I_{1:3}}$  are of type signed i.e.  $\iota s_{I_{1:3}} \in \{-1, +1\}^3$  and the symbol  $s_{I_4}$  is of type (unit) interval i.e.  $\iota s_{I_4} \in [-1, +1]$ , so that  $\mathbf{x}_{1,0}$  also writes as:

$$\mathbf{x}_{1,0} = \frac{1}{2}|\pm|_{I_1} + \frac{1}{4}|\pm|_{I_2} + \frac{1}{8}|\pm|_{I_3} + \frac{1}{8}\square_{I_4}. \quad (35)$$

$$\mathbf{x}_{2,0} = \frac{1}{2}|\pm|_{J_1} + \frac{1}{4}|\pm|_{J_2} + \frac{1}{8}|\pm|_{J_3} + \frac{1}{8}\square_{J_4}. \quad (36)$$

$\mathbf{x}_{2,0}$  is obtained analogously from  $J = [!(3, \mathbf{s}); !(1, \mathbf{i})]$  ( $I \cap J = \emptyset$ ) and  $\mathbf{x}_{2,0} = 15 + 1.Z_s^3(J)$  as in (33). The e-polynotope (or e-zonotope) related to the s-polynotope  $\mathbf{x}_{1,0}$  (or s-zonotope since  $E = \mathcal{I}$ ) is thus  $\mathcal{P}\mathbf{x}_{1,0} = \mathcal{Z}\mathbf{x}_{1,0} = 15 \pm 1$  (corollary 23). The independence of  $\mathbf{x}_{1,0}$  and  $\mathbf{x}_{2,0}$  coming from  $I \cap J = \emptyset$  gives (34). The polynotope  $\mathbf{x}_0 = [\mathbf{x}_{1,0}; \mathbf{x}_{2,0}]$  contains all the

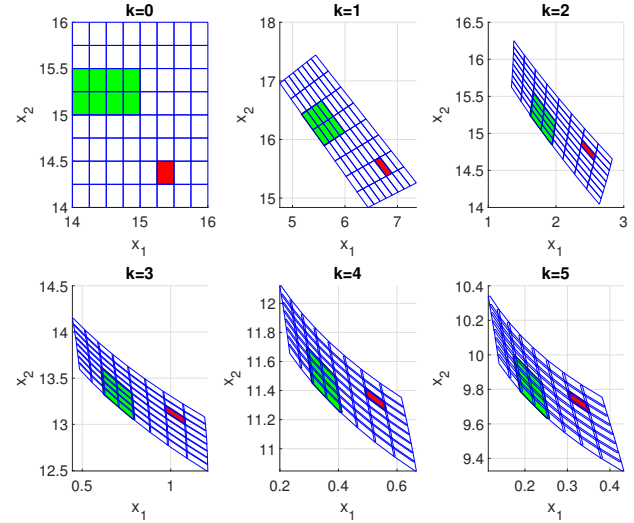


Fig. 6. Reachable sets resulting from a 3-level signed-interval mixed encoding of the initial states of a Lotka-Volterra model. The mixed polynotope computed at each time  $k$  characterizes (overlapping) outer approximations of the propagation of each of the 64 cells (red) paving the initial state set *with no bisection*. This also works with cell groups (green).

information required to decompose the initial state set  $[[14, 16]; [14, 16]]$  into a paving as in Fig. 6 for  $k = 0$ . Moreover, assigning values +1 or -1 to evaluate some of (or all) the signed symbols in (35)-(36) makes it possible to query about the range covered under some conditional values of signed symbols. This feature makes it possible to trace how each cell and/or cell groups within the “implicit paving” of the initial state set will propagate. It is worth underlining that this can be achieved *without any bisection*, only through the polynomial computations implementing the basic polynotope operators.

For the sake of illustration, an Euler sampling of the Lotka-Volterra model is considered:  $x_+ = x + f(x, 0)h$ , where the time index  $k$  is omitted,  $x_+$  stands for  $x_{k+1}$ , and the step size is  $h = 0.15s$ . The reduction operator  $\downarrow_{50}$  is applied at each iteration. The reachability analysis reported in Fig. 6 results from  $N = 5$  iterations starting from the initial state (32)-(33) satisfying (34). Let  $[+-+]$  be a short notation for  $[+1; -1; +1]$  (also applying for other sign combinations). Let  $\mathbf{x}|(s_I = v)$  denote the s-polynotope obtained by substituting in  $\mathbf{x}$  the expressions in  $v$  for the symbolic variables in  $s_I$ . Unless  $v$  depends on some symbols in  $s_I$ ,  $\mathbf{x}|(s_I = v)$  does not depend anymore on  $s_I$ . The related e-polynotope (resp. e-zonotopic enclosure) is  $\mathcal{P}\mathbf{x}|(s_I = v)$  (resp.  $\mathcal{Z}\mathbf{x}|(s_I = v)$ ). Considering the vectors of unique symbol identifiers  $I$  and  $J$  as in (35)-(36), the red (resp. green) cell at  $k = 0$  in Fig. 6 corresponds to  $\mathcal{P}\mathbf{x}_0|(s_{I_{1:3}} = [+ - +], s_{J_{1:3}} = [ - - +])$  (resp.  $\mathcal{P}\mathbf{x}_0|(s_{I_1} = [-], s_{J_{1:2}} = [+ -])$ ). Then, the single s-polynotope  $\mathbf{x}_k$  computed at each iteration  $k$  contains all the information required to obtain the related subplot

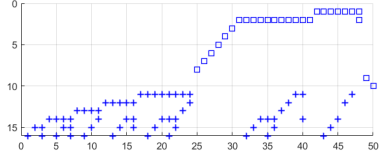


Fig. 7. Sparse structure of the exponent matrix  $E$  of  $\mathbf{x}$  at  $k = 5$ : 16 symbolic variables (interval:  $\square$  marks, signed:  $+$  marks), 50 monomials/generators, 90 non-zero elements.

in Fig. 6. In particular, the red (resp. green) zonotopic sets are  $\mathcal{Z}\mathbf{x}_k|_{(s_{I_{1:3}} = [+ - +], s_{J_{1:3}} = [- - +])}$  (resp.  $\mathcal{Z}\mathbf{x}_k|_{(s_{I_1} = [-], s_{J_{1:2}} = [+ -])}$ ) for  $k = 1, \dots, 5$ . These zonotopic enclosures are guaranteed to enclose the set of states reached from the initial red cell (resp. green cells) by iterating the sampled non-linear dynamics. Moreover, the initial ‘‘implicit paving’’ gradually leads to possibly overlapping cells (see the blue borders in Fig. 6) since the complexity of the polynotope computed at each iteration is reduced to a finite number (50) of generators. The sparse structure of the exponent matrix  $E$  of  $\mathbf{x}$  at  $k = 5$  is given in Fig. 7. The monomials involve 16 symbolic variables (10 of type unit interval: square marks, 6 of type signed:  $+$  marks). There are 90 non-zeros elements. The maximum degree is 3. As expected from the propagation of the initial mixed-encoding of states through a non-linear dynamic, several mixed monomials can be observed, that is, monomials involving both continuous and discrete symbolic variables.

This example of reachability with a mixed-encoding of state sets illustrates the ability of mixed polynotopes to trace the propagation of a significant number of hierarchically organized cells within non-trivial dynamics. Bissections have been avoided by dealing with polynomial dependencies between symbolic variables of different types combining continuous and discrete value domains. Moreover, the ability to explicitly characterize the overlapping between cells forming a partition of the initial state set paves the way for efficient symbolic abstraction techniques.

#### 7.4.2 Non-linear and mixed filtering with PKF

The Polynotopic Kalman Filter (PKF) developed in section §6 is applied to the modified Lotka-Volterra dynamic without and with a mixed encoding of states:

$$x_+ = x + \mathbf{f}(x, u)h + E\bar{v}, \quad (37)$$

$$y = x_1 + F\bar{w}. \quad (38)$$

The prediction model (37) (resp. measurement equation (38)) correspond to (19) (resp. (20)) in the formulation of PKF with  $v = [\bar{v}; \bar{w}]$  and  $\Phi = \mathcal{I}$ . The step size is  $h = 0.04$  and  $k \in \{0, \dots, N\} \subset \mathbb{N}$  with  $N = 750$  iterations. The initial and final times are  $t_0 = 0$  and  $t_f = Nh = 30$ . The input is  $u = 2$  for  $t \in [10, 20[$  i.e.  $250 \leq k < 500$ , and  $u = 0$  otherwise.  $E = 3.10^{-3}\mathcal{I}$ ,  $F = 1.5$ . The state

Table 6  
Computation times for 750 iterations of PKF in seconds (s). Cases: continuous ( $g = 0$ ) vs. mixed ( $g = 2$ ), and  $\downarrow_{50}$  vs.  $\downarrow_{100}$ .

|           | $g = 0$ | $g = 2$ |
|-----------|---------|---------|
| $q = 50$  | 3.4s    | 3.8s    |
| $q = 100$ | 13.9s   | 14.8s   |

and measurement noises are assumed to be bounded as  $\bar{v} \in [-1, +1]^2$  and  $\bar{w} \in [-1, +1]$  i.e.  $\mathcal{P}\mathbf{v} = [-1, +1]^3$ . The initial state set is assumed to be bounded by  $\mathcal{P}\mathbf{x}_0 = [[5, 25]; [5, 25]] \subset \mathbb{R}^2$ . These bounds are obtained from:

$$\begin{aligned} \mathbf{x}_{1,0} &= 15 + 10.Z_s^g([!(g, \mathbf{s}); !(1, \mathbf{i})]), \\ \mathbf{x}_{2,0} &= 15 + 10.Z_s^g([!(g, \mathbf{s}); !(1, \mathbf{i})]), \\ \mathbf{v} &= [Z_s^0([!(1, \mathbf{i})]); Z_s^0([!(1, \mathbf{i})]); Z_s^g([!(g, \mathbf{s}); !(1, \mathbf{i})])], \end{aligned}$$

where  $g$  stands for the granularity level of a mixed encoding of the initial states and the measurement noise at each sample time  $k$ . Two cases are considered:

- i)  $g = 0$  corresponds to a purely continuous case (solid lines in Fig. 8) with only symbols of type unit interval.
- ii)  $g = 2$  corresponds to a mixed case (dashed lines in Fig. 8) involving symbols of different types (signed and interval) in mixed polynotope computations.

At each iteration of PKF, the reduction operator  $\downarrow_q$  with  $q = 50$  or  $q = 100$  is used to: a) implement the reduction of  $\mathbf{x}$  as in (24), b) reduce the product  $\mathbf{x}_1\mathbf{x}_2$  in  $\mathbf{f}(\mathbf{x}, \mathbf{u})$ ; this is the only (inclusion preserving) difference between  $f$  (19) and  $\tilde{f}$  (25) in this example. Notice also that  $g$  (20) equals  $\tilde{g}$  (26) since the measurement/innovation equation (38) is linear. The simulation of the ‘‘true’’ system is obtained from  $x_0 = [22; 8]$  using Heun’s method. Consistently with (38), only the first state  $x_1 \in \mathbb{R}$  is measured at each sample time  $k$ , and the main purpose of PKF is to estimate state bounds  $\mathcal{B}\mathbf{x}$  for the state  $x \in \mathbb{R}^2$  while minimizing the (predicted) polynotope covariation trace. The computation times with a Matlab implementation are reported in Table 6: The mixed encoding does not increase very significantly the computation time in spite of the number of discrete configurations, contrary to the number of generators. The simulation results reported in Fig. 8 show a significant improvement of accuracy compared to EZGKF in a purely bounded-error setting with  $q = 200$  generators as in [14]. In particular, PKF shows an enhanced ability to reconstruct  $x_2$  from noisy measurements of  $x_1$ . Mixed encoding tends to give results with increased accuracy, especially for  $x_1$ , provided the number of generators is sufficient. Meanwhile, the maximum degree of computed polytopes is decreased from 6 (resp. 7) in the continuous case  $g = 0$  with  $q = 50$  (resp.  $q = 100$ ) to only 4 in both mixed cases i.e.  $g = 2$  with  $q = 50$  or 100. This is consistent with the reduced size of remainder intervals for  $g = 2$  and the influence of rewriting rules, in particular the inclusion neutral rule (11). This illustrates the ability of PKF to efficiently deal with nonlinear and mixed dynamics.

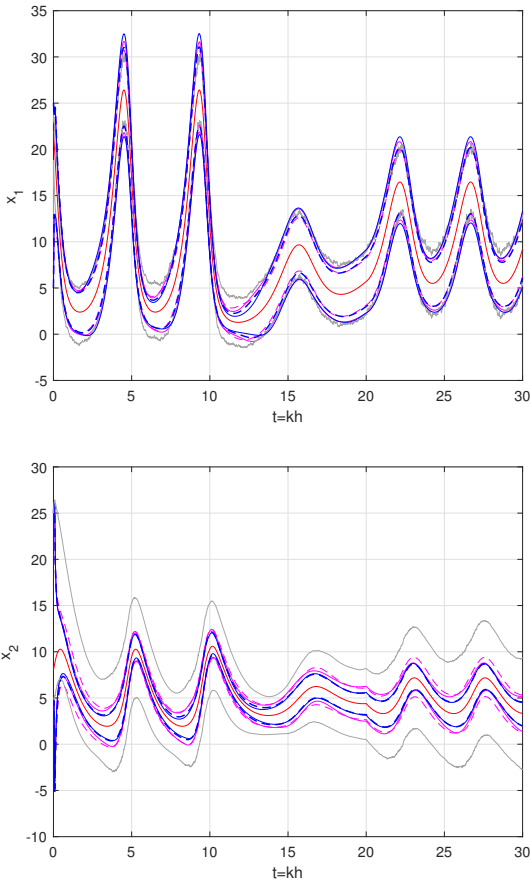


Fig. 8. Estimated state bounds vs. “true” values (red) of  $x_1$  (top) and  $x_2$  (bottom) with the Lotka-Volterra model: PKF with continuous (solid lines) or mixed (dashed lines) polynotopes, and  $\downarrow_{50}$  (magenta) or  $\downarrow_{100}$  as reduction operator. Comparison with EZGKF in a bounded-error setting (grey).

## 8 Conclusion

A framework for functional sets with typed symbols is introduced in this work. An explicit distinction between syntax and semantics helps formalize the management of dependencies, characterize sources of conservatism and analyze the impact of evaluation strategies (inner first vs. outer first/lazy/call-by-need). Image-sets with typed symbols generalize several set-representations like zonotopes and polynomial zonotopes to mixed domains, as exemplified with mixed polynotopes. The combination of polynomial functions with interval, signed and boolean symbolic variables through simple rewriting rules makes it possible to gather in a single compact and efficient data structure the description of non-convex and non-connected sets which would usually require costly bisection/splitting strategies to be propagated. The mixed-encoding of intervals proposed in this context allows to tune the granularity level of the discrete part of the description and, meanwhile, control the combinatorial complexity through the use of reduc-

tion operators. In addition, the traceability of uniquely identified typed symbols paves the way for advanced mixed sensitivity analysis and symbolic abstraction techniques. The reachability results show the relevance of the proposed framework to deal with the verification and synthesis of Cyber-Physical Systems (CPS). Based on modeling tools for nonlinear hybrid systems, a compositional implementation of advanced reachability and filtering algorithms is made possible by simply using operator overloading. This has been exemplified with the proposed Polynotopic Kalman Filter (PKF) which paves the way to advanced hybrid nonlinear filtering techniques preserving inclusion. Moreover, several bridges with random variables and stochastic filtering have been outlined as well as bridges with functional programming and object oriented paradigms, robust (and interpretable?) artificial intelligence [48,22] with the neural network activation function ReLU, sensitivity analysis, and symbolic abstractions of hybrid systems. Much remains to be done to exploit these connections.

## Acknowledgements

The author would like to thank Prof. Ali Zolghadri for many insightful discussions during this research work and for his careful reading of the manuscript.

## References

- [1] Teodoro Alamo, José M. Bravo, and Camacho Eduardo F. Guaranteed state estimation by zonotopes. *Automatica*, 41:1035–1043, 2005.
- [2] Amr Alanwar, Hazem Said, and Matthias Althoff. Distributed secure state estimation using diffusion kalman filters and reachability analysis. In *2019 IEEE 58th Conference on Decision and Control (CDC)*. IEEE, dec 2019.
- [3] Matthias Althoff. Reachability analysis of nonlinear systems using conservative polynomialization and non-convex sets. In Calin Belta and Franjo Ivancic, editors, *Proceedings of the 16th international conference on Hybrid systems: computation and control, HSCC 2013, April 8-11, 2013, Philadelphia, PA, USA*, pages 173–182. ACM, 2013.
- [4] Matthias Althoff and Bruce H. Krogh. Zonotope bundles for the efficient computation of reachable sets. In *Proceedings of the 50th IEEE Conference on Decision and Control and European Control Conference, CDC-ECC 2011, Orlando, FL, USA, December 12-15, 2011*, pages 6814–6821. IEEE, 2011.
- [5] Matthias Althoff and Bruce H. Krogh. Reachability analysis of nonlinear differential-algebraic systems. *IEEE Trans. Autom. Control*, 59(2):371–383, 2014.
- [6] Martin Berz and Kyoko Makino. Rigorous reachability analysis and domain decomposition of taylor models. In Alessandro Abate and Sylvie Boldo, editors, *Numerical Software Verification - 10th International Workshop, NSV 2017, Heidelberg, Germany, July 22-23, 2017, Proceedings [collocated with CAV 2017]*, volume 10381 of *Lecture Notes in Computer Science*, pages 90–97. Springer, 2017.
- [7] Dines Bjørner and Klaus Havelund. 40 years of formal methods. In *Lecture Notes in Computer Science*, pages 42–61. Springer International Publishing, 2014.

[8] José Manuel Bravo, Antonio Suárez, Manuel Vasallo, and Teodoro Alamo. Slide window bounded-error time-varying systems identification. *IEEE Trans. Autom. Control*, 61(8):2282–2287, 2016.

[9] Christophe Combastel. A state bounding observer based on zonotopes. *European Control Conference, ECC 2003*, pages 2589–2594, 2003.

[10] Christophe Combastel. A state bounding observer for uncertain non-linear continuous-time systems based on zonotopes. *Proceedings of the 44th IEEE Conference on Decision and Control, and the European Control Conference, CDC-ECC '05*, 2005:7228–7234, 2005.

[11] Christophe Combastel. Stable interval observers in C for linear systems with time-varying input bounds. *IEEE Transactions on Automatic Control*, 58(2):481–487, 2013.

[12] Christophe Combastel. Merging Kalman filtering and zonotopic state bounding for robust fault detection under noisy environment. *IFAC-PapersOnLine*, 28(21):289–295, 2015.

[13] Christophe Combastel. Zonotopes and Kalman observers: Gain optimality under distinct uncertainty paradigms and robust convergence. *Automatica*, 55:265–273, may 2015.

[14] Christophe Combastel. An extended zonotopic and gaussian kalman filter (EZGKF) merging set-membership and stochastic paradigms: Toward non-linear filtering and fault detection. *Annual Reviews in Control*, 42:232–243, 2016.

[15] Christophe Combastel and Sid-Ahmed Raka. On computing envelopes for discrete-time linear systems with affine parametric uncertainties and bounded inputs. *IFAC Proceedings Volumes (IFAC-PapersOnline)*, 44:4525–4533, 2011.

[16] Christophe Combastel, Qinghua Zhang, and Sid-Ahmed Raka. On using distorted sensors for set-based multi-scale actuator fault diagnosis. *IFAC Proceedings Volumes (IFAC-PapersOnline)*, 44:12015–12023, 2011.

[17] Christophe Combastel and Ali Zolghadri. A distributed Kalman filter with symbolic zonotopes and unique symbols provider for robust state estimation in CPS. *International Journal of Control*, (0):1–17, 2019.

[18] Thach Ngoc Dinh, Frédéric Mazenc, Zhenhua Wang, and Tarek Raïssi. On fixed-time interval estimation of discrete-time nonlinear time-varying systems with disturbances. In *2020 American Control Conference, ACC 2020, Denver, CO, USA, July 1-3, 2020*, pages 2605–2610. IEEE, 2020.

[19] Nicolas Ellero, David Gucik-Derigny, and David Henry. An unknown input interval observer for LPV systems under  $l_2$ -gain and  $l_\infty$ -gain criteria. *Automatica*, 103:294–301, 2019.

[20] Mirko Fiacchini, Teodoro Alamo, and Eduardo F. Camacho. On the computation of convex robust control invariant sets for nonlinear systems. *Automatica*, 46(8):1334–1338, aug 2010.

[21] Luiz Henrique De Figueiredo and Jorge Stolfi. Affine arithmetic: Concepts and applications. *Numerical Algorithms*, 37(1-4):147–158, 2004.

[22] Timon Gehr, Matthew Mirman, Dana Drachsler-Cohen, Petar Tsankov, Swarat Chaudhuri, and Martin Vechev. AI2: Safety and robustness certification of neural networks with abstract interpretation. In *2018 IEEE Symposium on Security and Privacy (SP)*. IEEE, may 2018.

[23] Antoine Girard. Reachability of uncertain linear systems using zonotope. In *Hybrid Systems: Computation and Control*, volume 3414 of *LNCS*, pages 291–305. Springer, 2005.

[24] Eric Goubault and Sylvie Putot. A zonotopic framework for functional abstractions. *Formal Methods in System Design*, 47(3):302–360, 2015.

[25] Eric Goubault and Sylvie Putot. Robust under-approximations and application to reachability of non-linear control systems with disturbances. *IEEE Control. Syst. Lett.*, 4(4):928–933, 2020.

[26] Branko Grnbaum. *Convex Polytopes*. Springer New York, New York, 2003.

[27] J. Roger Hindley and Jonathan P. Seldin. *Lambda-Calculus and Combinators, an Introduction*. Cambridge University Press, 2008.

[28] Fabian Immler, Matthias Althoff, Xin Chen, Chuchu Fan, Goran Frehse, Niklas Kochdumper, Yangge Li, Sayan Mitra, Mahendra Singh Tomar, and Majid Zamani. ARCH-COMP18 category report: Continuous and hybrid systems with nonlinear dynamics. In Goran Frehse, Matthias Althoff, Sergiy Bogomolov, and Taylor T. Johnson, editors, *ARCH18. 5th International Workshop on Applied Verification of Continuous and Hybrid Systems, ARCH@ADHS 2018, Oxford, UK, July 13, 2018*, volume 54 of *EPiC Series in Computing*, pages 53–70. EasyChair, 2018.

[29] Luc Jaulin, Michel Kieffer, Olivier Didrit, and Eric Walter. *Applied interval analysis*. Springer, 2001.

[30] Rudolf E. Kalman. A new approach to linear filtering and prediction problems. *Transactions of the ASME - Journal of Basic Engineering*, 82:35–45, 1960.

[31] Niklas Kochdumper and Matthias Althoff. Representation of polytopes as polynomial zonotopes. *arXiv:1910.07271*.

[32] Niklas Kochdumper and Matthias Althoff. Sparse polynomial zonotopes: A novel set representation for reachability analysis. *arXiv:1901.01780*, 2019.

[33] Niklas Kochdumper and Matthias Althoff. Constrained polynomial zonotopes. *arXiv:2005.08849*, 2020.

[34] Dirk P. Kroese, Tim Brereton, Thomas Taimre, and Zdravko I. Botev. Why the monte carlo method is so important today. *Wiley Interdisciplinary Reviews: Computational Statistics*, 6(6):386–392, jun 2014.

[35] Wolfgang Kühn. Rigorously computed orbits of dynamical systems without the wrapping effect. *Computing*, 61:pp. 47–67, 1998.

[36] Alex Kurzhanskiy and Pravin Varaiya. Ellipsoidal techniques for reachability analysis of discrete-time linear systems. *IEEE Trans. on Automatic Control*, 52(1):26–38, 2007.

[37] Vu Tuan Hieu, Cristina Stoica, Teodoro Alamo, Eduardo F. Camacho, and Didier Dumur. Zonotopic guaranteed state estimation for uncertain systems. *Automatica*, 49:3418–3424, 2013.

[38] Colas Le Guernic and Antoine Girard. Reachability analysis of linear systems using support functions. *Nonlinear Analysis: Hybrid Systems*, 4(2):250–262, 2010.

[39] Youdong Lin and Mark A. Stadtherr. Validated solutions of initial value problems for parametric odes. *Appl. Numer. Math.*, 57:1145–1162, 2007.

[40] Rudolf J. Lohner. *Perspectives on enclosure methods*, chapter On the ubiquity of the wrapping effect in the computation of error bounds, pages 201–216. Springer, Berlin, 2001.

[41] Moussa Maiga, Nacim Ramdani, Louise Travé-Massuyès, and Christophe Combastel. A comprehensive method for reachability analysis of uncertain nonlinear hybrid systems. *IEEE Trans. Autom. Control*, 61(9):2341–2356, 2016.

[42] Kyoko Makino and Martin Berz. Rigorous integration of flows and odes using taylor models. In Hiroshi Kai, Hiroshi Sekigawa, Tateaki Sasaki, Kiyoshi Shirayanagi, and Ilias S. Kotsireas, editors, *Symbolic Numeric Computation, SNC '09, Kyoto, Japan - August 03 - 05, 2009*, pages 79–84. ACM, 2009.

[43] D. G. Maksarov and J. P. Norton. Computationally efficient algorithms for state estimation with ellipsoidal approximations. *International Journal of Adaptive Control and Signal Processing*, 16(6):411–434, 2002.

[44] Frédéric Mazenc and Olivier Bernard. Interval observers for linear time-invariant systems with disturbances. *Automatica*, 47(1):140–147, 2011.

[45] Pierre-Jean Meyer, Alex Devonport, and Murat Arcak. TIRA : Toolbox for interval reachability analysis. In *Proc. of the 22nd ACM Int. Conf. on Hybrid Systems: Computation and Control*. ACM, apr 2019.

[46] Thomas Le Mezo, Luc Jaulin, and Benoit Zerr. An interval approach to compute invariant sets. *IEEE Transactions on Automatic Control*, 62(8):4236–4242, aug 2017.

[47] Mario Milanese and Carlo Novara. Set membership identification of nonlinear systems. *Automatica*, 40:957–975, 2004.

[48] Matthew Mirman, Timon Gehr, and Martin T. Vechev. Differentiable abstract interpretation for provably robust neural networks. In Jennifer G. Dy and Andreas Krause, editors, *Proc. of the 35th Int. Conf. on Machine Learning, ICML 2018, Stockholm, Sweden, July 10-15, 2018*, volume 80 of *Proceedings of Machine Learning Research*, pages 3575–3583. PMLR, 2018.

[49] Ian M. Mitchell. The flexible, extensible and efficient toolbox of level set methods. *J. Sci. Comput.*, 35(2-3):300–329, 2008.

[50] Marcelo Moisan, Olivier Bernard, and Jean-Luc Gouzé. Near optimal interval observers bundle for uncertain bioreactors. *Automatica*, 45(1):291–295, 2009.

[51] Ramon E. Moore. *Interval analysis*. Prentice-Hall, Englewood Cliffs, N.J., 1966.

[52] Nedialko S. Nedialkov, Ken R. Jackson, and George F. Corliss. Validated solutions of initial value problems for ordinary differential equations. *Applied Mathematics and Computation*, 105(1):21–68, 1999.

[53] Luis Orihuela, Pablo Milln, Samira Roshany-Yamchi, and Ramn A. Garca. Negotiated distributed estimation with guaranteed performance for bandwidth-limited situations. *Automatica*, 87:94–102, 2018.

[54] Luis Orihuela, Samira Roshany-Yamchi, Ramn A. Garca, and Pablo Milln. Distributed set-membership observers for interconnected multi-rate systems. *Automatica*, 85:221–226, 2017.

[55] Masoud Pourasghar, Christophe Combastel, Vicen Puig, and Carlos Ocampo-Martinez. FD-ZKF: A zonotopic Kalman filter optimizing fault detection rather than state estimation. *Journal of Process Control*, 73:89–102, 2019.

[56] Luc Pronzato. Optimal experimental design and some related control problems. *Automatica*, 44(2):303–325, feb 2008.

[57] Vicenç Puig, Jordi Saludes, and Joseba Quevedo. Worst-case simulation of discrete linear time-invariant interval dynamic systems. *Reliable Computing*, 9(4):251–290, 2003.

[58] Djahid Rabehi, Nacim Meslem, and Nacim Ramdani. Secure interval observer for linear continuous-time systems with discrete measurements subject to cyber-attacks. In *4th Conf. on Control and Fault Tolerant Systems, SysTol 2019, Casablanca, Morocco, Sept. 18-20, 2019*, pages 336–341. IEEE, 2019.

[59] Tarek Raïssi, Denis Efimov, and Ali Zolghadri. Interval state estimation for a class of nonlinear systems. *IEEE Trans. on Automatic Control*, 57(1):260–265, 2012.

[60] Tarek Raïssi and Denis V. Efimov. Some recent results on the design and implementation of interval observers for uncertain systems. *Automatica*, 66(3):213–224, 2018.

[61] Nacim Ramdani, Nacim Meslem, and Yves Candau. A hybrid bounding method for computing an over-approximation for the reachable set of uncertain nonlinear systems. *IEEE Trans. Autom. Control*, 54(10):2352–2364, 2009.

[62] Wolfgang Rautenberg. *A concise introduction to mathematical logic*. Springer New York, 2010.

[63] Raul Rojas. A tutorial introduction to the lambda calculus. *arXiv:1503.09060*, 2015.

[64] Damiano Rotondo, Andrea Cristofaro, Tor Arne Johansen, Fatiha Nejjari, and Vicenç Puig. State estimation and decoupling of unknown inputs in uncertain LPV systems using interval observers. *Int. J. Control*, 91(8):1944–1961, 2018.

[65] Siegfried M. Rump and Masahide Kashiwagi. Implementation and improvements of affine arithmetic. *Nonlinear Theory and Its Applications, IEICE*, 6(3):341–359, 2015.

[66] Fred C. Schweppe. Recursive state estimation: unknown but bounded errors and system inputs. *IEEE Trans. on Automatic Control*, 13(1):22–28, 1968.

[67] Dana S. Scott. Lambda calculus then and now. In *ACM Turing Centenary Celebration on - ACM-TURING 2012*. ACM Press, 2012.

[68] Joseph K. Scott and Paul I. Barton. Bounds on the reachable sets of nonlinear control systems. *Automatica*, 49(1):93–100, 2013.

[69] Joseph K. Scott, Davide M. Raimondo, Giuseppe Roberto Marseglia, and Richard D. Braatz. Constrained zonotopes: A new tool for set-based estimation and fault detection. *Automatica*, 69:126–136, jul 2016.

[70] François-Régis Sinot. Complete laziness: A natural semantics. *Electronic Notes in Theoretical Computer Science*, 204:129–145, apr 2008.

[71] Rihab El Houda Thabet, Tarek Raïssi, Christophe Combastel, Denis Efimov, and Ali Zolghadri. An effective method to interval observer design for time-varying systems. *Automatica*, 50(10):2677–2684, 2014.

[72] Ye Wang, Sorin Olaru, Giorgio Valmorbida, Vicenç Puig, and Gabriela Cembrano. Set-invariance characterizations of discrete-time descriptor systems with application to active mode detection. *Automatica*, 107:255–263, 2019.

[73] Feng Xu, Vicenç Puig, Carlos Ocampo-Martinez, Sorin Olaru, and Florin Stoican. Set-theoretic methods in robust detection and isolation of sensor faults. *Int. J. Syst. Sci.*, 46(13):2317–2334, 2015.

[74] Günter M. Ziegler. *Lectures on Polytopes*. Graduate Texts in Mathematics. Springer-Verlag, New York, NY, 1995.